

# **Seismic Profiling to Map Hydrostratigraphy in the Red Hill Area**

**RED HILL BULK FUEL STORAGE FACILITY  
JOINT BASE PEARL HARBOR-HICKAM, O‘AHU, HAWAI‘I**

**Administrative Order on Consent in the Matter of Red Hill Bulk Fuel Storage  
Facility, EPA Docket Number RCRA 7003-R9-2015-01 and  
DOH Docket Number 15-UST-EA-01, Attachment A, Statement of Work  
Section 6.2, Section 7.1.2, Section 7.2.2, and Section 7.3.2**

**March 30, 2018  
Revision 00**



**Comprehensive Long-Term Environmental Action Navy  
Contract Number N62742-12-D-1829, CTO 0053**

This page intentionally left blank

1 **Seismic Profiling to Map**  
2 **Hydrostratigraphy in the Red Hill**  
3 **Area**

4 **RED HILL BULK FUEL STORAGE FACILITY**  
5 **JOINT BASE PEARL HARBOR-HICKAM, O‘AHU, HAWAI‘I**

6 **Administrative Order on Consent in the Matter of Red Hill Bulk Fuel Storage**  
7 **Facility, EPA Docket Number RCRA 7003-R9-2015-01 and**  
8 **DOH Docket Number 15-UST-EA-01, Attachment A, Statement of Work**  
9 **Section 6.2, Section 7.1.2, Section 7.2.2, and Section 7.3.2**

10 **March 30, 2018**  
11 **Revision 00**

12 Prepared for:

13 **Defense Logistics Agency Energy**  
14 **8725 John J Kingman Rd Suite 4950**  
15 **Fort Belvoir, VA 22060-6222**

16 Prepared by:

17 **Lee Liberty and James St. Clair**  
18 **Department of Geosciences, Boise State University**  
19 **Boise, ID 83725-1536**

20 as: Technical Report BSU CGISS 18-01

21 for:

22 **AECOM Technical Services, Inc.**  
23 **1001 Bishop Street, Suite 1600**  
24 **Honolulu, HI 96813-3698**

25 Prepared under:



26 **Comprehensive Long-Term Environmental Action Navy**  
27 **Contract Number N62742-12-D-1829, CTO 0053**  
28

This page intentionally left blank

# Seismic profiling to map hydrostratigraphy in the Red Hill area, Oahu, Hawaii

Lee Liberty and James St. Clair

Department of Geosciences

Boise State University

Boise, Idaho 83725-1536

208-426-1166

[lliberty@boisestate.edu](mailto:lliberty@boisestate.edu)

Technical Report BSU CGISS 18-01

Friday, March 30, 2018

This page intentionally left blank

1 Contents

2 Summary ..... 1

3 Setting ..... 2

4 Approach ..... 5

5     Seismic imaging in volcanic terranes ..... 6

6     Seismic refraction method ..... 7

7         Inversion methods and uncertainty ..... 8

8     Seismic reflection ..... 10

9     Seismic data processing ..... 10

10     Uncertainty estimates for reflector depths ..... 12

11 Seismic transect results and interpretations ..... 13

12     Transect A ..... 14

13     Transect B ..... 17

14     Transect C ..... 20

15     Transect D ..... 22

16     Transect E ..... 25

17     Transect F ..... 28

18     Transect G ..... 31

19     Transect H ..... 33

20     Transect I ..... 35

21 Conclusions ..... 38

22 References ..... 39

23 Figures

24 Figure 1. Halawa/Red Hill area overview map ..... 3

25 Figure 2. Generalized geologic map (from Sherrod et al., 2007) with the seismic survey locations color  
26 coded by data acquisition type ..... 4

27 Figure 3. Schematic of seismic waves that travel through the subsurface ..... 5

28 Figure 4. Seismic shot gathers along Transect G ..... 9

29 Figure 5. Shot gather from Transect A ..... 10

30 Figure 6. Land-streamer-derived field gathers along Transect D ..... 12

31 Figure 7. Northwest to southeast Transect A refraction results ..... 15

32 Figure 8. Transect A refraction and reflection results ..... 16

1 Figure 9. Northwest to southeast Transect B refraction results..... 18

2 Figure 10. Transect B reflection and refraction profile..... 19

3 Figure 11. Northwest to southeast Transect C refraction results..... 20

4 Figure 12. Transect C reflection and refraction profile..... 21

5 Figure 13. North to south Transect D refraction results..... 22

6 Figure 14. Transect D reflection and refraction profile ..... 24

7 Figure 15. North to south Transect E refraction results ..... 26

8 Figure 16. Transect E reflection and refraction profile..... 27

9 Figure 17. North to south Transect F refraction results ..... 28

10 Figure 18. Transect F reflection and refraction profile ..... 30

11 Figure 19. West to east Transect G refraction results ..... 31

12 Figure 20. Transect G reflection and refraction profile ..... 32

13 Figure 21. West to east Transect H refraction results ..... 34

14 Figure 22. Transect H reflection and refraction profile ..... 35

15 Figure 23. West to east Transect I refraction results..... 36

16 Figure 24. Transect I reflection and refraction profile..... 37

1 Summary

2 We present the results from nine seismic profiles acquired in the Red Hill area of Oahu, Hawaii (Figure 1)  
3 over a nine-day acquisition window in December, 2017. The seismic objectives were to map stratigraphy  
4 and hydrogeologic boundaries beneath three valleys to the north of Honolulu, Hawaii; North Halawa  
5 Valley (Transects A, B and C), South Halawa Valley (Transects D, E, F, and G) and Moanalua Valley  
6 (Transects H and I). Seismic data quality were generally very good with: 1) clear first arrivals needed to  
7 obtain shallow seismic velocity distributions and 2) observable reflections noted between surface wave  
8 and seismic refraction signals to map large-contrast subsurface boundaries. Seismic refraction results  
9 constrain seismic velocities for the upper 100 feet and tie those velocities to nearby well logs and to  
10 other published results from Hawaii in order to help constrain travel time to depth conversions for the  
11 seismic reflection results. Seismic reflection results show the geometry and depth to key  
12 hydrostratigraphic boundaries within the upper 1,000 feet below land surface. Key reflectors include the  
13 base of alluvium or top of saprolite, top of water saturated (possibly perched) sediments, and the  
14 contact between weathered basalt (saprolite) and unweathered basalt.

15 Alluvium that represents mobilized and transported valley fill sediments are constrained to the upper 60  
16 feet below land surface in all three valleys. Saturated and/or competent saprolite (chemically weathered  
17 basalt) are mapped from surface to hundreds of feet depth. Our observations are consistent with v-  
18 and/or u-shaped saprolite base geometries across the valleys with the maximum saprolite thickness  
19 below surface stream flow locations. The saprolite base extends to hundreds of feet below sea level in  
20 North and South Halawa Valleys. The depth to saprolite base was constrained by only one short profile  
21 beneath Moanalua Valley. The depth to these key hydrostratigraphic boundaries in South Halawa Valley  
22 are consistent with lithologic log interpretations from nearby monitoring wells. The seismic images do  
23 not provide insight into the geometry or depth to regional or basal water table, in part due to shallow  
24 and confined perched water systems and the lack of large physical property contrasts (seismic velocity  
25 and density) at this basal water system boundary. The seismic images also do not constrain volcanic  
26 stratigraphy (e.g., individual volcanic flows, lava tubes) beneath the top of unweathered basalt unit due  
27 to complexities in the seismic wavefield within this layered basalt system. This report summarizes the  
28 first known seismic reflection survey that identifies and characterizes the saprolite base for the deeply  
29 incised valleys of the Hawaiian Islands (Figure 2).

1 Setting

2 The axis of North Halawa, South Halawa, and Moanalua Valleys all trend northeast-southwest and  
3 extend from the crest of the Ko’olau Range (Figure 1, Izuka, 1992). Rainfall ranges from an annual  
4 average of 150 inches in the upper valley to 40 inches in the lower valley (Blumenstock and Price, 1967).  
5 Izuka (1992) described North Halawa Valley as a narrow, V-shaped valley that has been carved by  
6 erosion where a colluvial apron lines the base of the valley walls and alluvium and saprolite (clayey,  
7 highly weathered basalt) lie above unaltered basaltic rocks. Newer monitoring wells show that adjacent  
8 valleys have similar volcanic-stratigraphic configurations. The three valleys are located on the leeward,  
9 southwestern flank of the Ko’olau Range where a thick sequence of thin lava flows from the  
10 approximately 2 million year old (Ma) Ko’olau volcanic series basalt dips under the overlying valley fill  
11 sediments (Figure 2). The Ko’olau volcanic series consists mostly of pāhoehoe and massive a’ā lava along  
12 with highly permeable a’ā clinker zones. Late-stage volcanic rejuvenation volcanic rocks (less than 2 Ma)  
13 of the Honolulu volcanic series are mapped at the southern portions of the study area. Chemical  
14 weathering of these basalts leads to enhanced saprolite formation beneath the gentle valley slopes with  
15 high precipitation rates and infiltration driving chemical processes (e.g., Hunt, 1996; Nelson et al., 2013).  
16 The transition from basalt to saprolite does not result in a significant change in rock volume, and often  
17 intact structures and the fabric of the source rock are observed within the saprolite. Weathered  
18 materials extend to below sea level along the transects surveyed across these valleys. The piezometric  
19 surface in the regional basalt aquifer in the vicinity of Red Hill is ranges from approximately 17.7 feet to  
20 22.4 feet above mean sea level (AECOM, 2017). Shallower piezometric levels are observed in valley fill  
21 and in saprolite within valleys. This suggests perched groundwater systems, or continuously saturated  
22 geologic sections, connecting the shallow system to the deeper regional groundwater system are  
23 common.

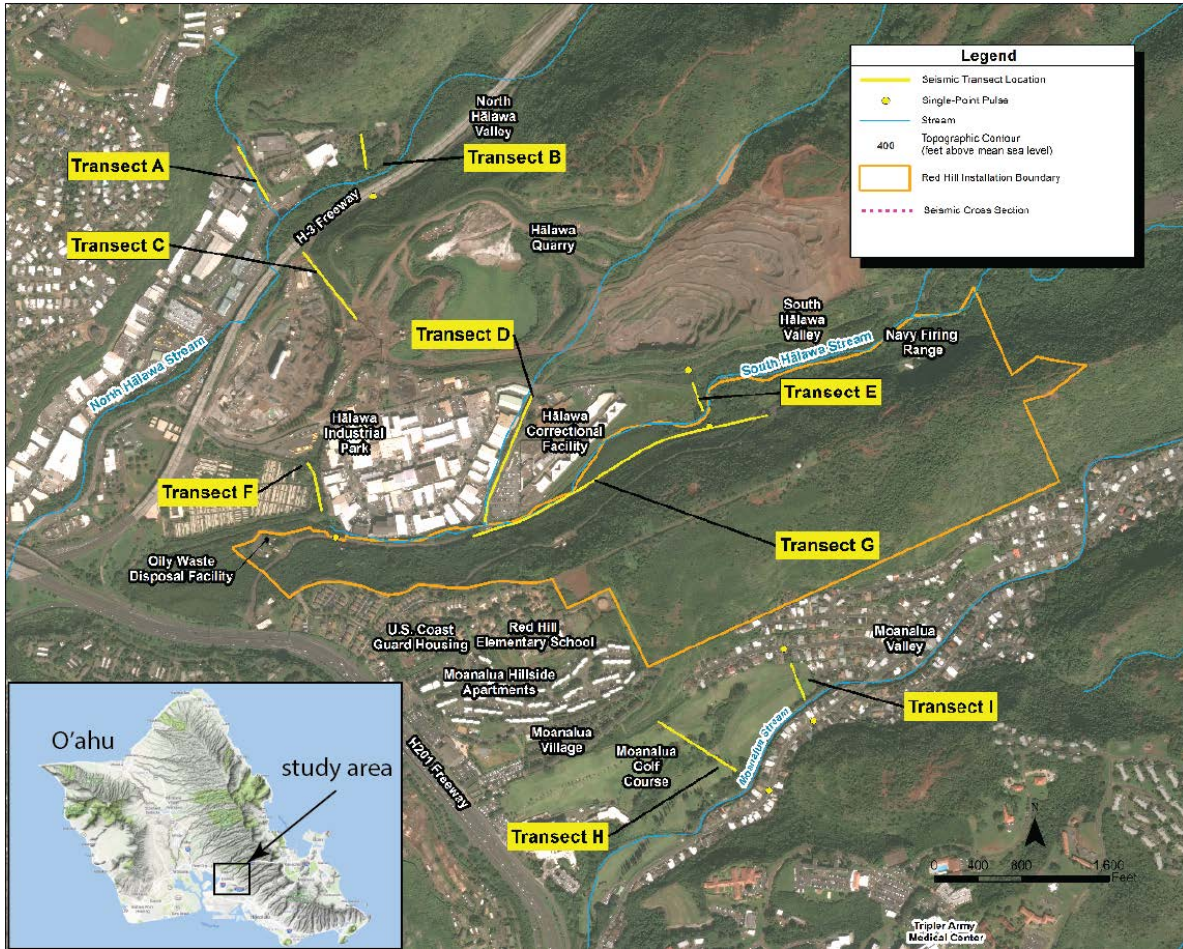


Figure 1. Halawa/Red Hill area overview map. The site is located in a heavily urbanized area north of Honolulu on the island of Oahu, Hawai'i. Nine seismic transects along three incised valleys are presented in this report.

1

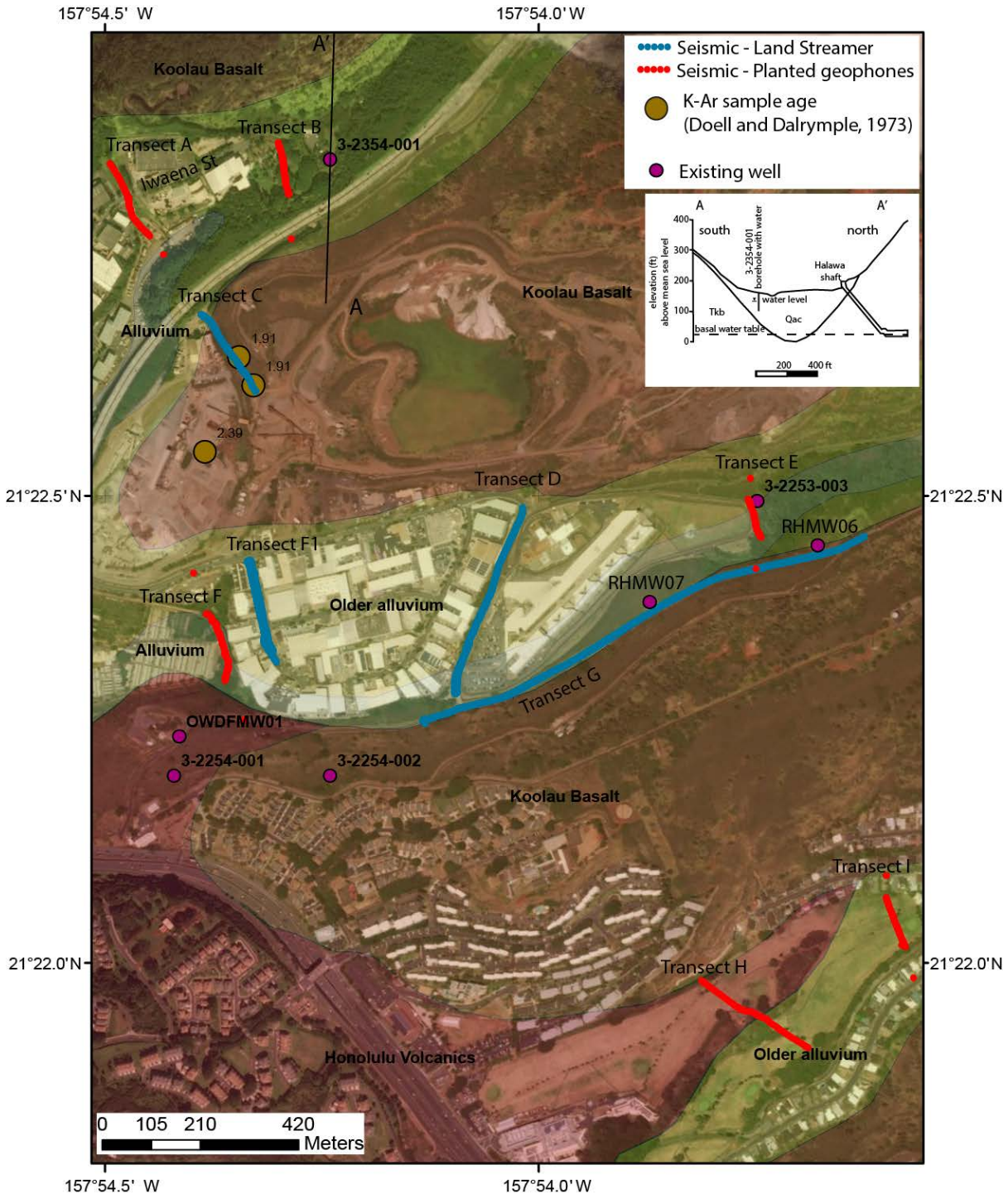
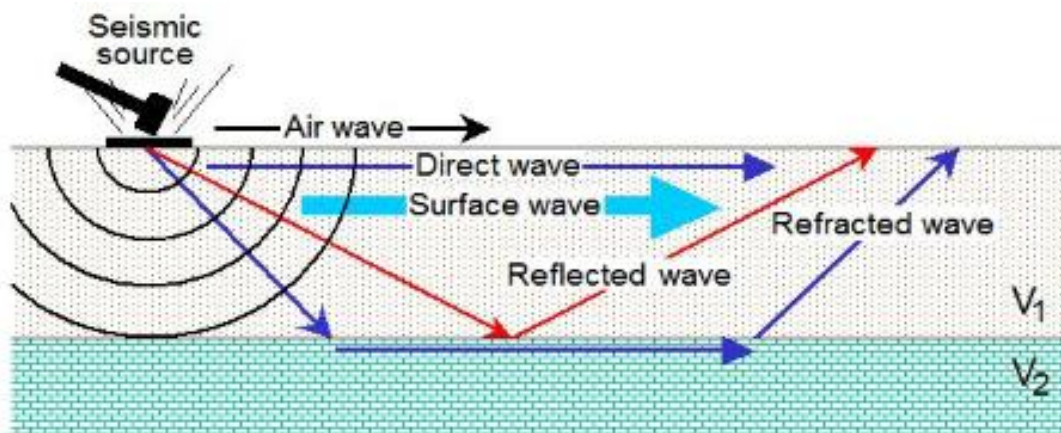


Figure 2. Generalized geologic map (from Sherrod et al., 2007) with the seismic survey locations color coded by data acquisition type. Ko’olau and Honolulu volcanic series rocks lie beneath the higher elevations while weathered basalts (saprolite) and alluvium occupy the low lying valleys. Cross section A-A’ across the North Halawa Valley (from Izuka, 1992) shows the general geometry of the valley fill (alluvium and saprolite) with respect to the underlying unaltered basalt.

1

## 1 Approach

2 Seismic imaging involves the use of sound waves to map the subsurface layers of the earth. This  
3 approach relies on the recording of returned seismic waves that travel along, and reflect at, geologic or  
4 hydrostratigraphic boundaries (Figure 3). To obtain seismic signals, we rely on a sound source (e.g.  
5 hammer) that hits the ground every few feet along the earth's surface. Sound waves travel into the  
6 earth in all directions (similar to throwing a stone in a pond and watching the waves traveling away from  
7 the source) and return to the land surface along a variety of travel paths (Figure 3) where the seismic  
8 signals are measured with ground motion sensors (geophones) spaced every few feet. The amplitude  
9 and travel time of the returns are recorded and digitized with a seismograph. We rely on many  
10 geophones to record and separate each sound wave return where the amplitude and travel time  
11 differences are used to build seismic velocity maps and subsurface images of reflecting boundaries  
12 (similar to using a sonogram to image the human body). The fastest (first) seismic arrival for each  
13 sounding and at each geophone location represents a direct or refracted wave while large amplitude  
14 reflected returns at later travel times mark contrasts in seismic velocity and/or rock densities at depth.  
15 Slower surface waves are also generated with this imaging approach, but these signals are removed for  
16 our analysis. Seismic source and geophone positions span each transect length to allow subsurface  
17 signals to be separated. For this study, we focused on reflected arrivals for the upper 1,000 feet and  
18 refracted arrivals for the upper 100 feet along nine transects in three valleys.



19 Figure 3. Schematic of seismic waves that travel through the subsurface. This report focuses on seismic reflection and refraction arrivals to estimate the material properties, depth, and geometry of key hydrostratigraphic boundaries.

20 Seismic surveys to map subsurface structures and stratigraphy are the current standard in many  
21 industries. This approach is the primary tool to identify and characterize oil and gas reserves, to  
22 characterize geologic structures, stratigraphy, and hazards, and to map key hydrostratigraphic  
23 boundaries for constraining numerical groundwater flow and transport models. Newer approaches have  
24 been adapted to image shallow targets (upper 1,000 feet) in urban settings and in complex volcanic  
25 terranes (e.g., Liberty, 2011; Liberty et al., 2015). Typically, seismic signals for the range of target depths  
26 can be obtained from an impulsive (hammer) or swept (vibroseis) seismic source and geophones planted  
27 into the ground with the use of 3-inch long spikes. Although vibroseis sources can be very effective in

1 urban environments, vehicle access can be difficult, deployment costs can be prohibitive, and  
2 acquisition times can increase due to long source occupations when compared to impulsive (accelerated  
3 hammer) sources. Thus, a hammer source was chosen for this survey.

4 In urban areas, land access can be difficult and surveys can be restricted to right of way access and along  
5 paved roads, thus transect locations are limited to obtaining proper permits along open and continuous  
6 stretches of land. A relatively new approach to imaging in urban settings is the use of seismic land  
7 streamer systems where geophones are coupled to the road surface via base plates and sources are  
8 quickly moved along the surface (Van der Veen and Green, 1998 and van der Veen et al., 2001). Results  
9 from these land streamers have produced results comparable to planted geophone surveys and access  
10 permits are often obtained from a single agency (e.g. City or County permit). Additionally, data  
11 collection rates using land streamers can be considerably faster and require fewer field personnel  
12 compared to geophone planting surveys, assuming straight roads or right-of-ways. For this survey, we  
13 used a 10 pound (lb) sledge hammer and PEG-40 accelerated weight drop  
14 (<https://rtclark.com/product/peg-40kg-propelled-energy-generator-5/>) source mounted to the hitch of a  
15 pickup truck. We used 10 Hertz (Hz) vertical planted and land streamer-based geophones to obtain both  
16 p-wave seismic reflection and refraction data in profile. We recorded between 72 and 120 channels for  
17 each transect with source and receiver positions spaced between 3 and 10 feet. These changing  
18 parameters were driven by field logistics (restricted profile lengths) with maximum target depths of  
19 1,000 ft. The distance from the source to the nearest receiver with the land streamer system was 30 ft  
20 and within a few feet for geophone planted transects. Kinematic global positioning system (GPS) survey  
21 information was provided for each geophone and source location. Source soundings were acquired  
22 between each geophone position and at select off-end shot locations.

### 23 Seismic imaging in volcanic terranes

24 Seismic imaging objectives are simplest where seismic velocities increase with depth and where lateral  
25 changes in those velocities are not complex. While relatively unaltered volcanic rock environments with  
26 interbedded basalts and sediments can result in complex seismic wavefields and velocity inversions, the  
27 incised valleys of Hawaii offer a relatively simple seismic velocity distribution (see Figure 2 inset).  
28 Whereas seismic energy can be trapped in the sediment or volcanic interbeds or voids in unaltered  
29 volcanic terranes (e.g., Liberty et al., 2015), the deep weathering profiles beneath Hawaiian valleys  
30 generally form a stratified seismic column that makes for a simpler imaging objective (e.g., Izuka, 1992).  
31 Thus, we anticipate an increase in velocity with depth from seismic arrivals beneath the valleys and  
32 strong reflectivity at large contrast (alluvium or saprolite base) boundaries.

33 Expected seismic velocities for this study area are summarized in Table 1. While unaltered basalt  
34 generally has a measured bulk seismic velocity of more than 3,000 meters per second (m/s) at  
35 atmospheric conditions, rock alteration or fracturing will decrease seismic velocities (Stanchits et al.,  
36 2006). Unaltered basalts are found at depth beneath the valleys and close to land surface beneath the  
37 adjacent hills (e.g., Hunt, 1996).

38 For the incised valleys of Hawaii, seismic velocities generally increase with depth (e.g., Yaede et al.,  
39 2015; Von Voigtlander et al., 2018). Typically, dry alluvium lies at the shallowest depths and for these  
40 depths, seismic waves travel through alluvium at relatively slow velocities. These mechanically  
41 transported lie upon chemically weathered basalts (saprolite) and/or saturated sediments. Seismic  
42 velocities for saprolite can span over a large range, but because saprolites represent differentially

1 weathered basalt they have seismic velocities typically greater than alluvium, but less than unaltered  
 2 basalt. The velocity of water saturated sediments generally exceeds the speed of sound in water (about  
 3 1,480 m/s) but is specifically dependent on porosity, water saturation, and lithology (e.g., Mavco et al.,  
 4 2009). For this survey, we define four lithologies with seismic velocities that increase with depth for the  
 5 materials beneath the three incised valleys (Table 1). We define: 1) dry alluvium or soil as less than  
 6 1,000 m/s (can be faster at greater depths due to compaction), 2) dry highly weathered basalt or  
 7 saprolite from 1,000-1,500 m/s, 3) saturated or hard saprolite from 1,500-3000 m/s and, 4) unaltered  
 8 basalt at seismic velocities greater than 3,000 m/s.

Lithology	Vp (m/s)	Vp (m/s) - alternate study
Dry alluvium/soil	< 1000 <sup>1</sup>	< 700 <sup>2</sup>
Saturated clays	1100-2500 <sup>3</sup>	
Saprolite	1000 - 1900 <sup>1</sup>	700 - 1200 <sup>2</sup>
Weathered/fractured basalt	1900 – 3000 <sup>1</sup>	1200 – 3000 <sup>2</sup>
Basalt	>3000 <sup>1</sup>	3000 <sup>4</sup> (at atmospheric pressure)

9 *Table 1. Seismic velocity estimates relevant to the study area. Velocities from <sup>1</sup>VonVoigtlander (2015),  
<sup>2</sup>Brandes et al. (2011) and <sup>3</sup>Mavco et al. (2009), <sup>4</sup>Stanchits et al (2006).*

10 Seismic refraction method

11 The seismic refraction method involves the recording of returned first arrival signals that either 1)  
 12 refract along high seismic velocity subsurface boundaries, or 2) dive to greater depths and return to the  
 13 surface at large distances, with respect to probing depth, in the presence of velocity gradients. P-wave  
 14 refraction surveys are a standard approach to finding: 1) the depth to the water table within  
 15 sedimentary layers; 2) the depth to bedrock beneath sedimentary layers; 3) the seismic velocity gradient  
 16 within sedimentary layers; and 4) the depth to multiple high contrast subsurface boundaries (e.g.,  
 17 Pelton, 2005). We use the travel-times of the first arrival energy from each shot point to each receiver to  
 18 estimate the seismic velocity distributions. In some cases, a clear break in seismic first arrivals can be  
 19 seen (e.g., Figure 3) that best represent hard seismic boundaries. Often, diving waves are observed  
 20 where a velocity gradient model best matches the observed seismic signals. For our interpretations, we  
 21 calculate seismic velocities using a cell size that ranged from 3-5 feet both along the profile and with  
 22 depth rely upon the steepness of velocity gradient with respect to depth to identify lithology changes.

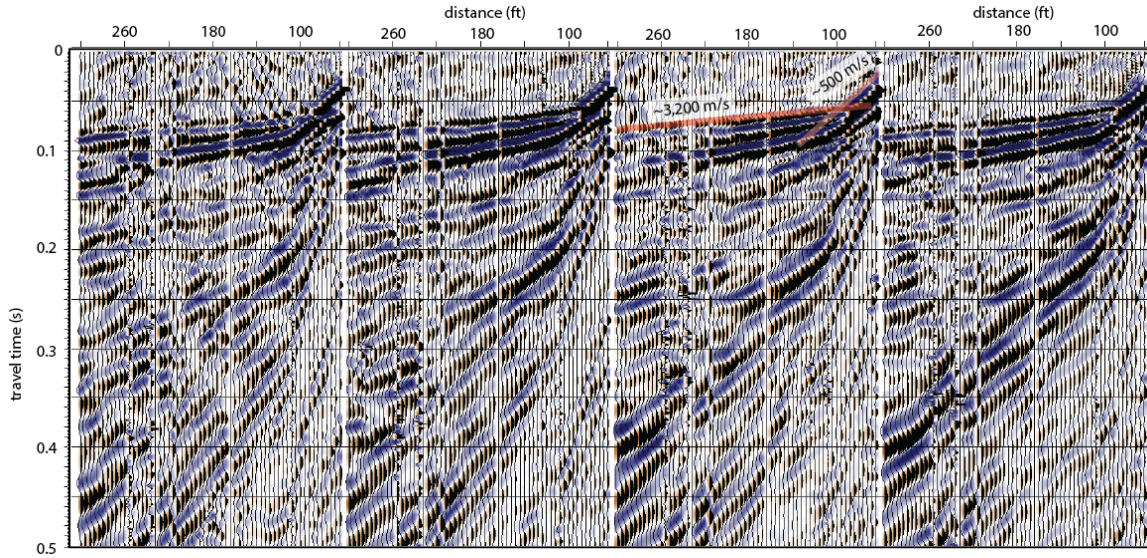
23 We identify the first arrival time as the first ground motion at each trace (Figures 4 and 5). We pick the  
 24 arrivals in two stages. Where the background noise obscures the first arrival time but the waveforms are  
 25 still easily observable, we select the first arrival time based on the lateral continuity of the first arriving  
 26 waveform across multiple traces for each shot gather. We initially pick the first arrivals on the raw data  
 27 and then apply a bandpass filter to suppress spurious noise signals to add to the pick database. This  
 28 filter does not shift travel time picks (a zero phase filter), but allows additional travel time picks in the  
 29 presence of noise. On traces where we did not confidently pick the first arrival, we did not make an  
 30 observation.

1 We were able to confidently pick first arrivals on most of shot gathers for both streamer and planted  
2 geophone surveys. The streamer data tend to be a little noisier than the planted phone data due to  
3 poorer geophone coupling with the road surface compared to geophones planted in firm ground.  
4 However, the land streamer transects have a greater shot density and thus the noisier dataset was  
5 offset by greater first arrival picks. Table 2 shows the number of travel-time observations for each  
6 transect as well as the percent of possible observations (from the total number of seismic traces). For  
7 the streamer lines, we picked between 30 and 59 percent of the data and for the planted phone surveys,  
8 we picked between 43 and 93 percent of the data. Due to the large data volume, there is significant  
9 redundancy in first arrival picks compared to a typical refraction survey where only a few shot records  
10 are used for analysis.

#### 11 Inversion methods and uncertainty

12 We use a travel-time tomography code (modified from St. Clair, 2015) to estimate the shallow velocity  
13 structure. The velocity model is parameterized as a mesh of constant velocity cells with a fixed  
14 horizontal width and a vertical thickness that increases with depth. The strategy is to generate a  
15 reasonable starting model and then alternate between: 1) ray-tracing to predict travel-times for the  
16 current model and 2) using a linearized inversion with smoothness constraints to map the residual  
17 travel-times (predicted – observed) into an updated model with a smaller root mean squared (RMS)  
18 misfit (e.g., Zelt et al., 2013). The process is terminated when RMS misfit between successive iterations  
19 becomes negligible (Figure 5). RMS misfits for each transect are listed in Table 2 and are on the order of  
20 our estimated pick uncertainty (2-3 milliseconds).

21 Quantifying model uncertainty and resolution of tomographic models is a difficult task because of the  
22 large number of models that need to be tested. Uncertainty tests that explore the relationship between  
23 starting models and final solutions can show standard deviations upwards of 25% for individual model  
24 parameters. Higher values (>15-20%) typically correspond to regions with strong velocity gradients or  
25 low ray coverage, but similar results are observed when comparing results from different algorithms  
26 (Zelt et al., 2013). Even in the presence of large uncertainties, large scale features such as depth to  
27 bedrock and strong lateral velocity changes tend to be well resolved using any refraction analysis  
28 approach.



1 Figure 4. Seismic shot gathers along Transect G. The first arrivals are identified and measured travel times for each geophone offset are used to build a seismic velocity model for the subsurface. Here, we identify a clear break in first arrival velocities that represents dry alluvium overlying basalt.

Transect	n-picks (% of total)	Final Model RMS misfit (ms)
A	5614 (72)	2.8
B	2222 (66)	2.5
C*	5125 (59)	1.4
D*	7750 (30)	2.7
E	7417 (93)	2.2
F	7608 (83)	1.4
G*	25575 (52)	2.5
H	3081 (43)	2.3
I	6549 (92)	1.9

2 Table 2. Number of travel-time picks for each transect and RMS misfit for velocity inversion. Asterisks  
 3 indicate land streamer profiles. Misfit is measured in milliseconds (ms).

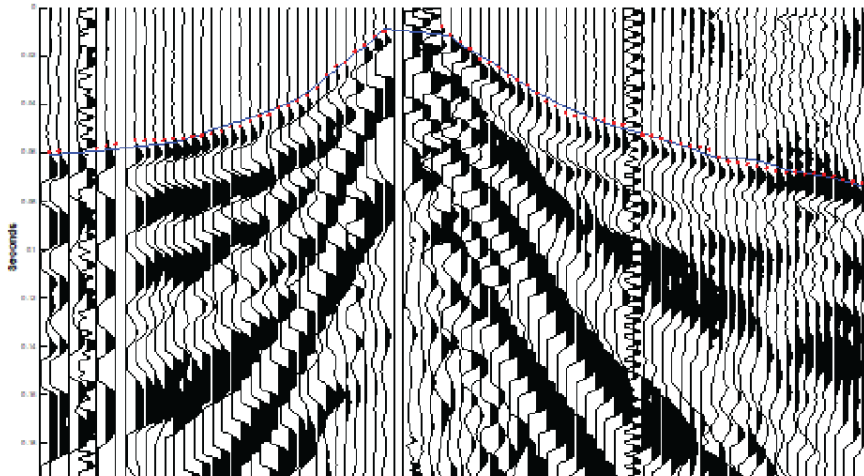


Figure 5. Shot gather from Transect A. First arrival picks are shown as red dots, blue curve shows predicted travel-times from velocity inversion.

1

2 Tomographic velocity models are best constrained in areas with many redundant and crossing raypaths.  
 3 To avoid interpreting unconstrained regions of the velocity models, we mask regions in the final  
 4 tomographic model with no ray coverage. We display the ray coverage using both a derivative weight  
 5 sum (DWS) map, which represents the sum of all ray segment lengths in each model cell, and a plot of  
 6 the raypaths.

#### 7 Seismic reflection

8 The seismic reflection method involves the recording of reflected returns (echoes) from subsurface  
 9 layers with the use of an impulsive (e.g., hammer) or swept (e.g., vibroseis) seismic source and an array  
 10 of geophone ground motion sensors. Because seismic energy is reflected at each subsurface location  
 11 where measureable changes in seismic velocity or density are present, this is a standard approach for  
 12 characterizing geologic stratigraphy, structure and the presence of fluids. The reflection method  
 13 requires dense and regularly spaced source soundings and receiver measurements. For this survey,  
 14 source and geophone spacing was 3-10 feet along the length of each transect. This spacing was mostly  
 15 driven by profile length restrictions associated with access or permitting requirements, or physical  
 16 barriers.

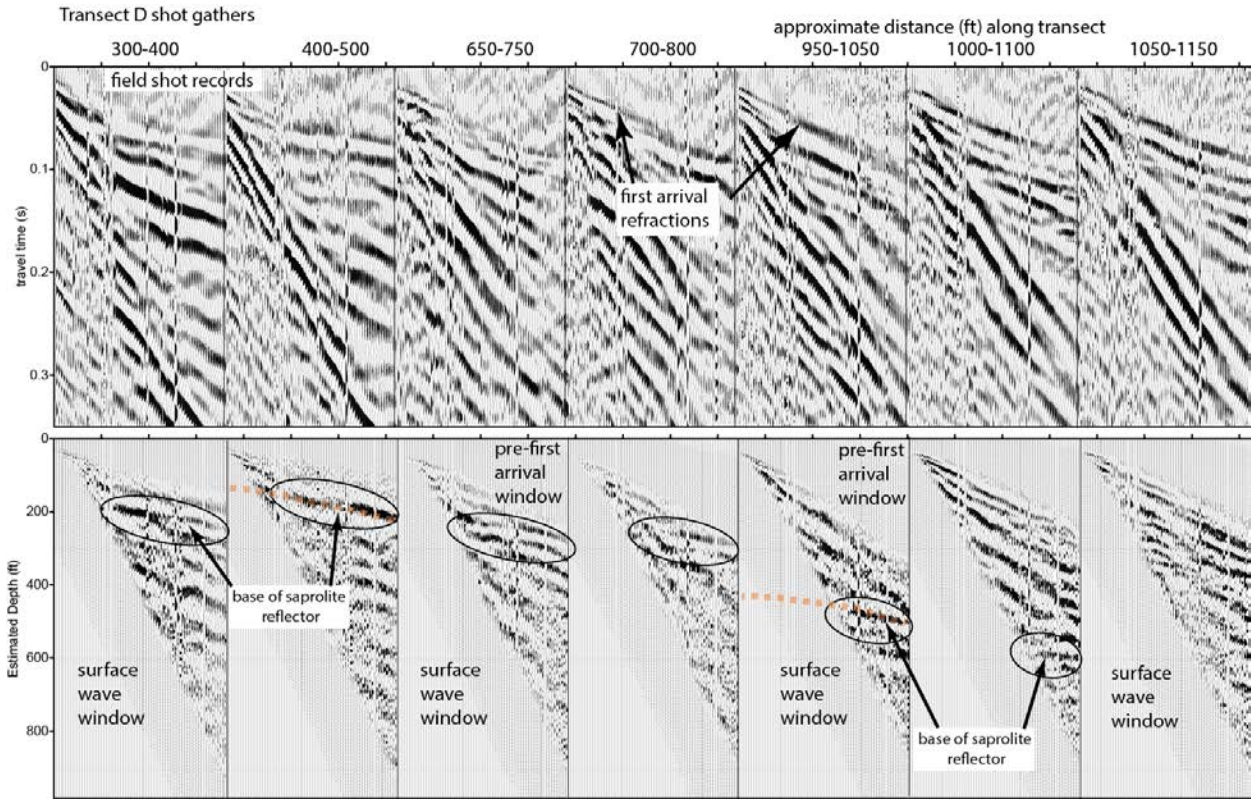
#### 17 Seismic data processing

18 The seismic reflection data processing involves a number of steps that are consistent with the Yilmaz  
 19 (2001) approach. We use Halliburton's SeisSpace® ProMAX® seismic processing software  
 20 (<https://www.landmark.solutions/SeisSpace-ProMAX>) for each processing step. We then use the open  
 21 source Seismic Unix utilities to produce final images. Figure 6 highlights both raw field records and  
 22 processed gathers from the ProMAX interface. Below is a summary of each processing step:

- 23 1) Assign each source and receiver location to a spatial position and elevation. We use universal  
 24 transverse Mercator (UTM) coordinates for each location. This is a convenient and universal  
 25 approach to spatially locate both field locations and final interpretation positions.
- 26 2) Identify and remove bad traces and/or shots. On occasion, a false trigger was recorded and  
 27 stored as a field record, Also, a geophone position was sometimes not recorded (e.g. on a street  
 28 crossing). These traces were removed from subsequent processing steps

- 1        3) Apply datum or elevation statics for each trace. We use a replacement velocity derived from  
2        refraction analysis for each transect that was consistent with near surface values. We select a  
3        datum near the maximum elevation for each profile.
- 4        4) Data sort from shot gathers to common midpoint (CMP) gathers. The CMP position is the  
5        midpoint between source and receiver locations for each trace. This step ensures that the  
6        subsurface reflectors are placed in the proper spatial position (but is dip independent).
- 7        5) Spiking deconvolution and filters to remove source signature and sharpen the seismic wavelet.  
8        This step is critical to identify and isolate reflection signals from other coherent signals  
9        (refractions, waveguides, surface waves, air wave). See Figure 6 for filter response.
- 10       6) Amplitude gains to counter spherical divergence and scattering (attenuation) effects. This step  
11       also helps normalize the reflection amplitudes with respect to other coherent noise signals.  
12       Amplitude gain windows were longer than the reflection window to ensure the relative seismic  
13       amplitudes were preserved.
- 14       7) Dip moveout (DMO) analysis to remove the reflector dip dependence in the subsequent velocity  
15       analysis. This is an iterative step with (8) and incorporates dip in identifying midpoint locations.  
16       This step is consistent with the Deregowski (1986) and Hale (1988) approach.
- 17       8) Velocity analysis to measure the best fit hyperbolic moveout at stacking seismic velocities as a  
18       function of travel time (depth) and CMP position. Once velocity analysis is complete, the DMO  
19       step (7) is repeated. This iterative process continues until there is no difference between  
20       measured stacking velocities between DMO iterations. See orange dashed lines on Figure 6 that  
21       show velocity hyperbolas on the processed gathers. Note that stacking velocities approximate  
22       the root mean square velocity average of all layers above the reflector.
- 23       9) Apply normal moveout (NMO) corrections derived from velocity and DMO analyses to remove  
24       the hyperbolic moveout and remove offset dependence for each CMP trace.
- 25       10) Top and bottom mutes to remove refracted arrivals and surface waves. Our top mute removes  
26       wavelet stretching of more than 50% from the NMO process to minimize wavelet distortion for  
27       shallow reflectors. Our bottom mute removes surface wave signals that remain after filter  
28       application. We found surface wave attenuation approaches did not reveal reflection signals  
29       within the ground roll window. Typically, signals with a slower velocity than the air wave (linear  
30       moveout of about 335 m/s) were muted or removed from subsequent processing.
- 31       11) Calculate and apply of residual statics. We rely on a maximum power autostatics approach that  
32       cross correlates each trace with a derived pilot (summed) trace (Ronen and Claerbout, 1985).  
33       Residual static shifts did not exceed  $\frac{1}{2}$  of the dominant seismic wavelength.
- 34       12) Common mid-point (CMP) stack. This process averages each source-receiver pair amplitude for  
35       each travel time that is located at the same CMP. A nominal 24-36 trace fold was obtained for  
36       each CMP position that is spaced 1.5-5 ft apart. For final stacks, we summed adjacent CMP  
37       positions to obtain a final CMP spacing that is equal to the shot spacing for each transect.
- 38       13) Post-stack FX-Deconvolution to remove random noise from the stack within the frequency range  
39       for reflection signals (Gulunay, 1986).
- 40       14) Kirchoff travel time migration to move reflectors to the proper spatial position (e.g., Vidale,  
41       1988). This process was not applied to high noise datasets because it tends to amplify noisy  
42       signals.
- 43       15) Travel time to depth conversion using constraints from refraction results and stacking velocities  
44       derived from steps 7 and 8 and from assumptions consistent with Dix equation conversions from

- 1 stacking velocities to interval velocities. We rely on constant stacking velocity gradients with
- 2 depth below the strongest reflector to estimate depth on the stacked images.
- 3 16) Stack display scaled for each trace with the largest amplitude representing the largest seismic
- 4 velocity or density contrast for approximately the upper 1000 ft.



5  
6 Figure 6. (top) land-streamer-derived field gathers along Transect D. The gather positions are consistent  
7 with the stacked image presented below. (bottom) filtered and muted gathers with an estimate of depth  
8 derived from velocity analysis. Each common mid point gather contains 36 traces from different  
9 source/receiver pairs that are summed along the curves derived from velocity analyses.

10 Uncertainty estimates for reflector depths  
11 In the absence of borehole seismic measurements, reflection arrival times for a range of source-receiver  
12 offsets provide the estimate of seismic velocity with depth and position. This measured velocity  
13 distribution, in turn, provides the conversion from travel time to depth for a final seismic image. The  
14 measured seismic velocity for a reflection represents an average rock velocity for the overlying layers.  
15 These velocity estimates are valid with the assumption of flat lying stratigraphy, a relatively simple rock  
16 velocity distribution (e.g., no anisotropy) with respect to seismic wavelengths, that primary seismic  
17 arrivals (not multiples) are arriving from within the (2D) imaging plane, and that a range of source-  
18 receiver offsets are obtained that are comparable to the target depths. The dip moveout process  
19 (described above) corrects the dip dependence of seismic velocity under the assumption of relatively  
20 simple geologic conditions (i.e., these assumptions fail with complex structures like salt domes or thrust  
21 fault environments where large zones of very slow rock velocities can underlie faster velocity rocks).

1 With increasing reflector depth, larger offsets are needed to obtain reliable travel time to depth  
 2 conversions via a velocity analysis. In general, reasonable seismic velocity information (within about  
 3 10%) can be obtained when the offsets are about ½ the target depths (with the assumptions noted  
 4 above). Thus, we suggest both seismic reflection and refraction imaging depths presented in the report  
 5 are accurate to within 10% of actual depths.

6 **Seismic transect results and interpretations**

7 The following section presents seismic results for seismic transects located in North Halawa Valley  
 8 (Transects A, B and C), South Halawa Valley (Transects D, E, and F) and Moanalua Valley (Transects H  
 9 and I). Table 3 is a summary of location, seismic source used, type of geophone, date of acquisition,  
 10 number of seismic channels, geophone and source spacing and the total number of shots for each  
 11 profile. We start by presenting the seismic refraction results that examine the seismic velocity  
 12 distributions for the upper 100 feet. We then present the seismic reflection results and integrate the  
 13 refraction results into a final interpretation.

Transect	Location	Valley	Source	Geophones	Date Acquired	Channels	spacing (feet)	Number of shots
A	Iwaena Street	North Halawa	PEG40/sledge	vertical	12/18/2017	120	6	797
B	Board Water Supply	North Halawa	PEG40/sledge	vertical	12/14/2017	90	4	99
C	Queen Emma Quarry	North Halawa	PEG40	streamer	12/16/2017	72	5	940
D	Correctional Facility Entrance Road	South Halawa	PEG40	streamer	12/15/2017	72	5	726
E	Correctional Facility Back Access Road	South Halawa	PEG40	vertical	12/12/2017	90	3	92
F	Animal Quarantine Entrance	South Halawa	PEG40	vertical	12/17/2017	96	5	241
F1	Waiua Street	South Halawa	PEG40	streamer	12/10/2017	72	5	797
G	Icarus Road	South Halawa	PEG40	streamer	12/13/2017	72	5	685
H	Moanalua Golf Course 1	Moanalua	sledge	vertical	12/11/2017	86	5	93
I	Moanalua Golf Course 2	Moanalua	PEG40	vertical	12/11/2017	88	4	90

14 *Table 3. Summary of seismic acquisition parameters for each transect. See Figures 1 and 2 for locations.*  
 15 *Note that Transect F1 was acquired by not analyzed due to conditions beneath the road surface that did*  
 16 *not produce usable signals. This profile will not be discussed in this report.*

## 1 Transect A

2 The northwest-southeast oriented 620 foot long Transect A seismic survey was acquired with planted  
3 geophones across North Halawa Valley along a property easement that extends along a south flowing  
4 tributary of North Halawa stream (Figures 1 and 2). The profile crosses Iwaena Street approximately 250  
5 ft from the northwest end of the profile and descends about 40 feet of elevation (Figure 7). Transect A  
6 terminates to the southeast (downhill) along a municipality service road for large service vehicles.  
7 Sledge hammer seismic shots were acquired along the profile to the north of Iwaena Street due to lack  
8 of vehicle access and PEG40 accelerated hammer hits were acquired along the southern half of the  
9 profile. Ko'olau volcanic series basalt (bedrock) outcrops appear a few hundred feet uphill (north) from  
10 the start of the survey (Sherrod et al., 2007) and the North Halawa stream is located immediately  
11 southeast of the profile termination. From previous models (e.g., Izuka, 1992), we expect bedrock  
12 depths to be greater along the southern portions of the profile.

13 The seismic refraction results from Transect A show a general increase in seismic velocities with depth,  
14 with surface velocities ranging from 400-1200 m/s, mostly consistent with dry soil or alluvium (Figure 7).  
15 At depths upwards of 30 feet, velocity increases are consistent with a transition from alluvium to dry  
16 saprolite. The shallow velocity distribution suggests a relatively constant alluvium thickness across the  
17 profile and no clear evidence for an incised North Halawa stream channel near its present day surface  
18 expression. Dry saprolite velocities are identified at the very northern portion of this profile at surface  
19 elevations, consistent with basalt/saprolite outcrops mapped about 300 feet to the north of the transect  
20 (Sherrod et al., 2007). Approximately 40 to 50 feet below land surface along most of the transect,  
21 seismic velocities exceed 1,500 m/s, consistent with either hard or saturated saprolite. This is the  
22 approximate depth that Izuka (1992) identified saturated saprolite in well 3-2354-001 (Figure 2) that is  
23 located approximately 1,300 feet upgradient of this transect (see inset map on Figure 2). The one area  
24 where the refraction data do not show velocities that exceed 1,500 m/s is located at distances between  
25 200 and 300 feet along the transect. Here, low velocities extend to the base of the refraction model,  
26 consistent with dry saprolite extending to greater depths. This lower velocity zone may represent a  
27 lateral break in the perched water system or it may represent a zone of less competent saprolite. We  
28 conceptualized a model of a dry zone beneath the central portion of the profile where shallow water fed  
29 by the north channel of the North Halawa Stream is providing perched water to the northern portions of  
30 the profile while the main North Halawa Stream channel is contributing to the perched system close to  
31 the current stream channel. At a depth of approximately 90 feet along the northern portion of the  
32 profile, seismic velocities exceed 3,000 m/s, the value that represents unaltered basalt at surface  
33 conditions (Stanchits et al, 2006). There is no evidence in the refraction results to suggest that velocities  
34 that represent unweathered basalt are present along other portions of the profile in the upper 100 feet  
35 below land surface.

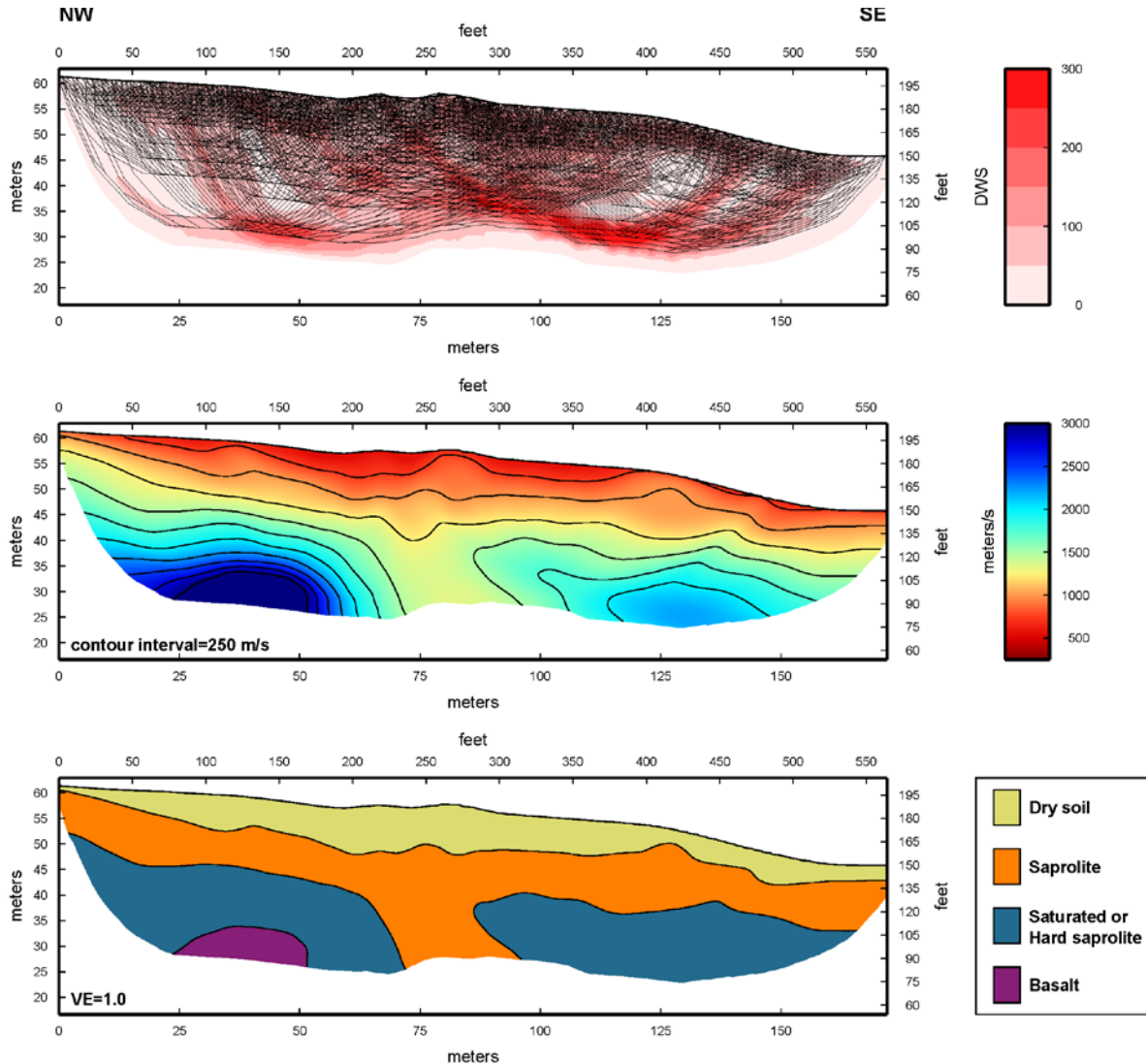


Figure 7. Northwest to southeast Transect A refraction results. (top) Derivative weight sum profile showing ray density for the refraction analysis. (middle) Inversion result showing velocity distribution along the profile. (bottom) Lithologic interpretation derived from velocity profile and from other published results from Hawaii.

1

2 At the depth that basalt is mapped along the northern portions of the seismic refraction profile (Figure  
 3 7), the seismic reflection profile shows a high amplitude ~30 degree southeast dipping reflector that we  
 4 interpret as the base of saprolite or top of unaltered basalt (Figure 8). This strong amplitude reflector  
 5 suggests that there is an abrupt seismic velocity and/or rock density contrast at this boundary along the  
 6 length of the profile that extends to approximately 400 feet below land surface or about 250 feet below  
 7 sea level. Along the profile, other large amplitude (and parallel) reflectors are noted and it is not clear  
 8 whether this pattern represents a more complex boundary at the saprolite base (e.g. multiple  
 9 saprolite/basalt transitions), whether we observe out-of-plane reflectors (perhaps representing  
 10 downgradient heterogeneities or an oblique seismic profile orientation with respect to geologic dip), or  
 11 whether we observed basalt stratigraphy beneath the saprolite base. Regardless, this reflection pattern

- 1 suggests a high contrast semi-continuous boundary that extends to a few hundred feet below sea level
- 2 along the length of the profile. At position 550 feet along the transect, the saprolite base reflector
- 3 abruptly changes dip direction and now slopes to the northwest. This reflector dip is poorly constrained
- 4 due to limited coverage at the southeast portion of this profile, but may represent the changing
- 5 saprolite base geometry at the center of the valley and beneath North Halawa Stream.

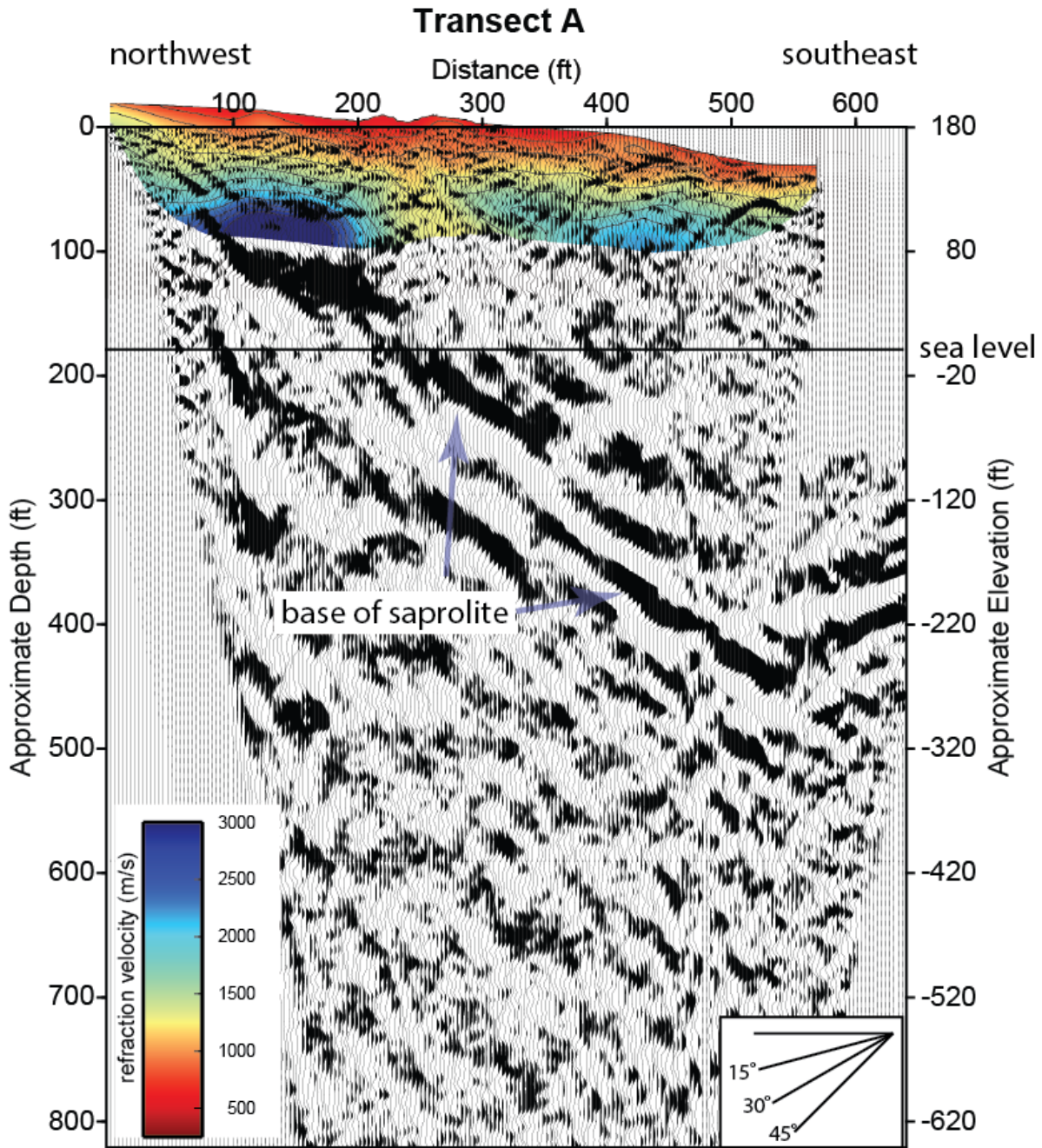


Figure 8. Transect A refraction and reflection results showing a southeast dipping saprolite base reflector. The axis of the basal reflector is noted at about the 550-foot position along the transect. Datum elevation is 180 feet.

## 1 Transect B

2 The 350 foot long northwest-southeast trending Transect B seismic survey was acquired with planted  
3 and land streamer geophones across North Halawa Valley on the Honolulu Board of Water Supply(BWS)  
4 Halawa Xeriscape garden property immediately north of the North Halawa stream (Figures 1 and 2). The  
5 profile is located along the garden access road along the northern portions of the profile and extends  
6 across a grass field and garden area to the south (Figure 9). The profile gradually decreases in surface  
7 elevation by about 30 feet to the south (Figure 9). Sledge hammer seismic shots were acquired along the  
8 southern portion of the profile and PEG40 accelerated hammer hits were acquired along the northern  
9 half of the profile. Ko'olau volcanic series basalt outcrops appear a few hundred feet uphill from the  
10 north end of the profile (Sherrod et al., 2007) and the North Halawa Stream and H3 highway are located  
11 immediately southeast of the profile termination. From the Izuka (1992) report, we expect to encounter  
12 basalt bedrock near sea level elevations, as is noted in well log 3-2354-001 that is located about 300 feet  
13 upgradient from the center of the profile (Figure 2). This report also noted perched water at  
14 approximately 40 to 50 feet below land surface in this well.

15 The seismic refraction results from Transect B show a general increase in seismic velocities with depth,  
16 with a higher velocity gradient observed along the southeastern portion of the profile (Figure 9). The  
17 surface velocities are generally less than 1,000 m/s, consistent with dry soil or alluvium. At depths  
18 between approximately 30 to 50 feet, velocity increases are consistent with a transition from alluvium  
19 to dry saprolite with a thicker zone of alluvium appearing beneath the central portion of the profile. The  
20 shallow velocity distribution is consistent with a deeper alluvial paleochannel across the center portion  
21 of the profile. We map dry saprolite velocities at the very northern portion of this profile at surface  
22 elevations, consistent with basalt/saprolite outcrops mapped immediately to the north of the transect  
23 (Sherrod et al., 2007). Approximately 35 feet below land surface along the southern portions of the  
24 profile seismic velocities exceed 1,500 m/s, consistent with either hard or saturated saprolite. This is the  
25 approximate depth that Izuka (1992) identified saturated saprolite in well 3-2354-001 (see inset map on  
26 Figure 2). Given the proximity of the southern portion of the profile to the modern North Halawa Creek  
27 and to well 3-2354-001, this high velocity zone is consistent with a perched or continuously saturated  
28 zone within saprolite. This interpretation is also consistent with the Transect A results where the region  
29 beneath the central portion of the profile is dry and saturated conditions are perhaps related to a  
30 tributary to the North Halawa Stream. We do not identify velocities along Transect B that exceed 3,000  
31 m/s, suggesting the absence of unaltered basalts, in the upper 100 feet below land surface along this  
32 profile. Seismic refraction velocities decrease along the very southern end of the profile, either related  
33 to poor ray coverage or an increase in depth to water saturation or stiffer saprolite.

34 The most prominent arrival on seismic reflection profile is a v-shaped reflector that extends to  
35 approximately 20 feet below sea level at transect position 175 (Figure 10). This reflector extends to  
36 within 50 feet of the surface near the ends of the profile, where high velocity refraction results suggest  
37 that this represents the base of saprolite. The refraction velocities do not quite reach 3,000 m/s below  
38 this reflector, but this may be simply related to poor velocity controls at the base of the refraction  
39 model. This depth of this reflector increases at the far southeastern portion of the profile where ray  
40 coverage is poor. The seismic reflection profile shows no persistent reflector related to the base of  
41 shallow alluvium, but does show shallow subparallel reflectors above the interpreted base of saprolite  
42 reflector. These reflectors may either represent out-of-plane reflectors or intact structure within the  
43 saprolite unit.

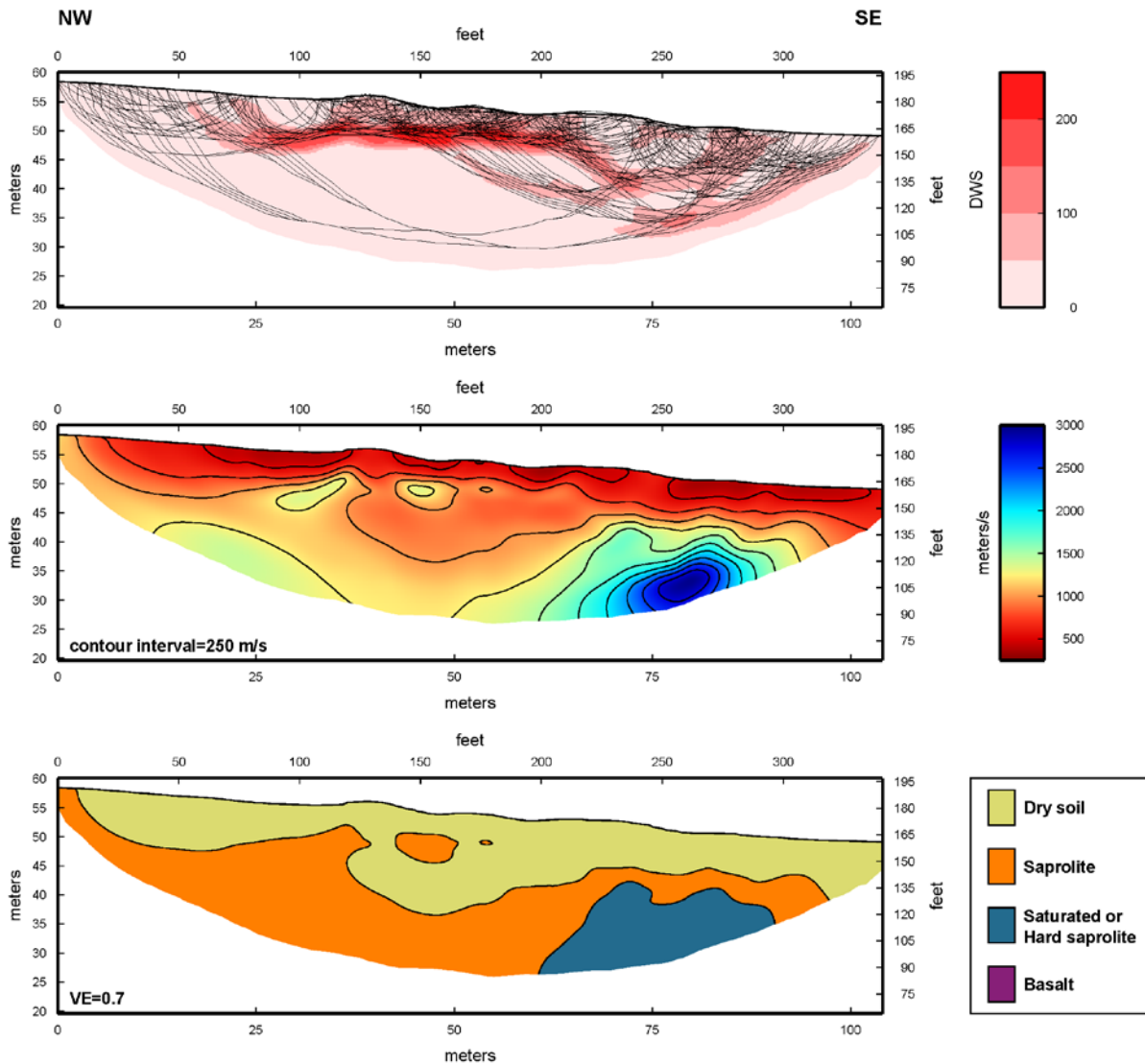


Figure 9. Northwest to southeast Transect B refraction results. (top) Derivative weight sum profile showing ray density for the refraction analysis. (middle) Inversion result showing velocity distribution along the profile. (bottom) Lithologic interpretation derived from velocity profile and from other published results from Hawaii.

1

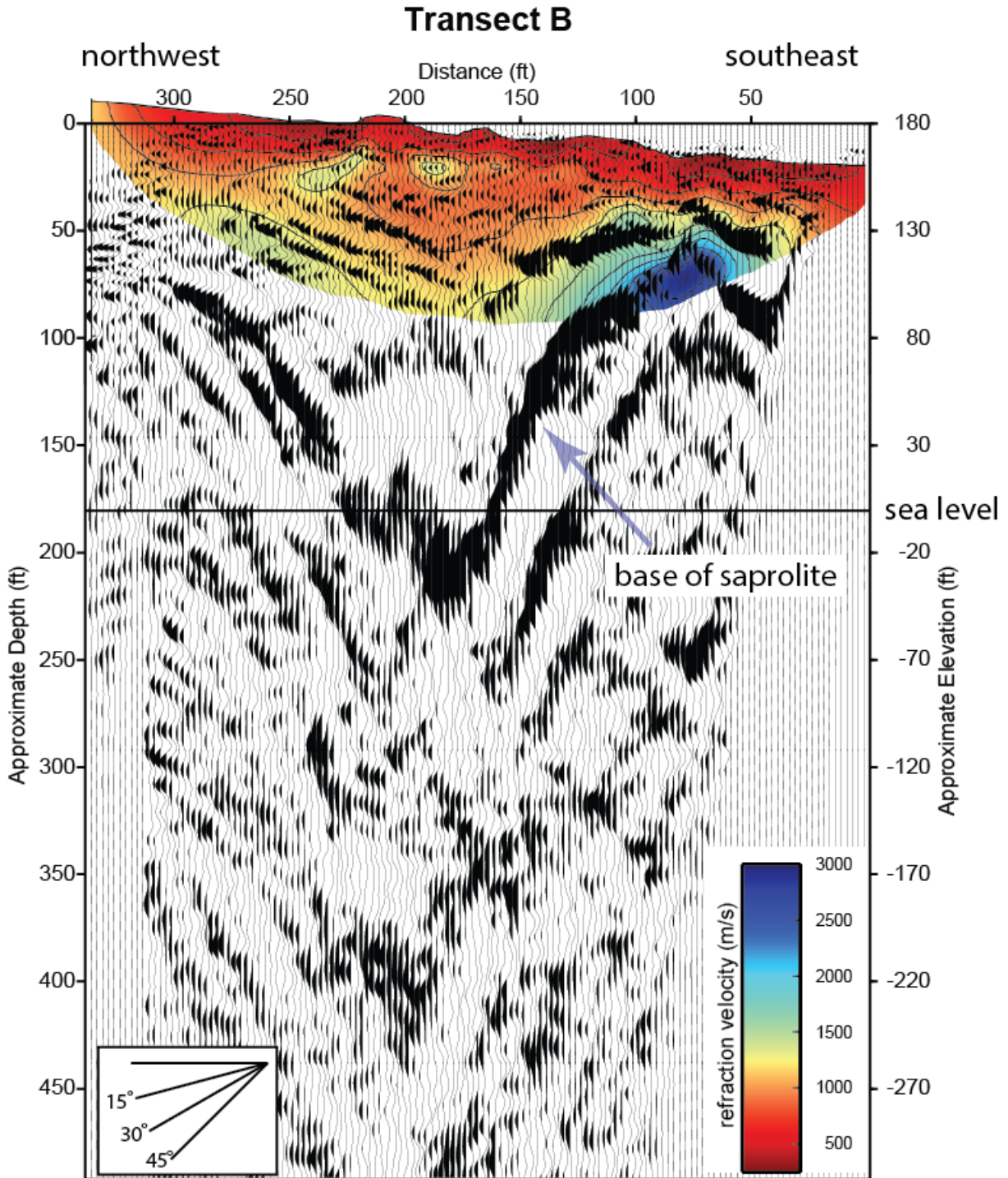
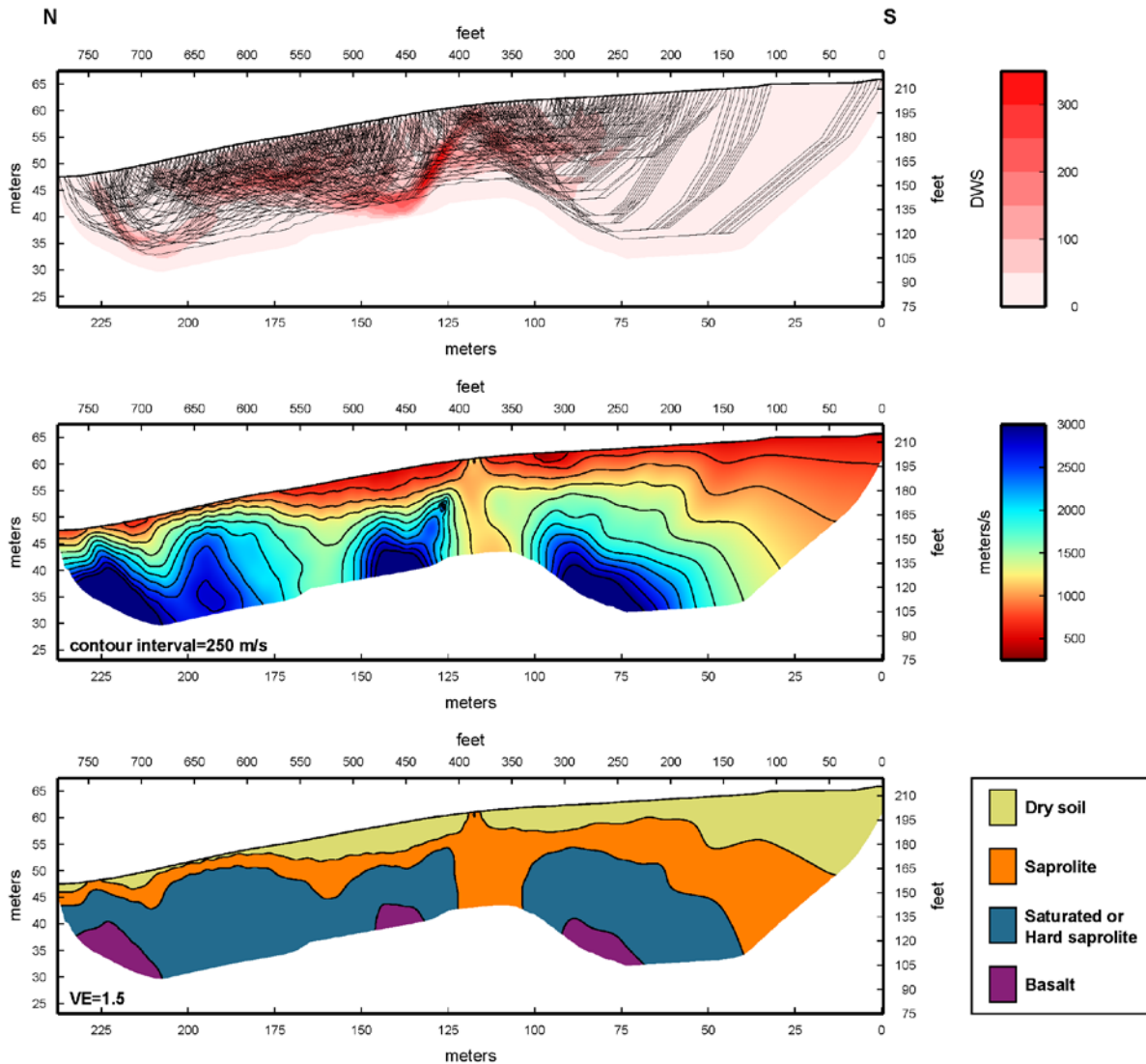


Figure 10. Transect B reflection and refraction profile showing the geometry of the saprolite base as a v-shaped reflector. The axis of the basal reflector is noted along the transect profile at approximately position 175 feet, and beneath the thickest zone of alluvium. Datum elevation is 180 feet.

1

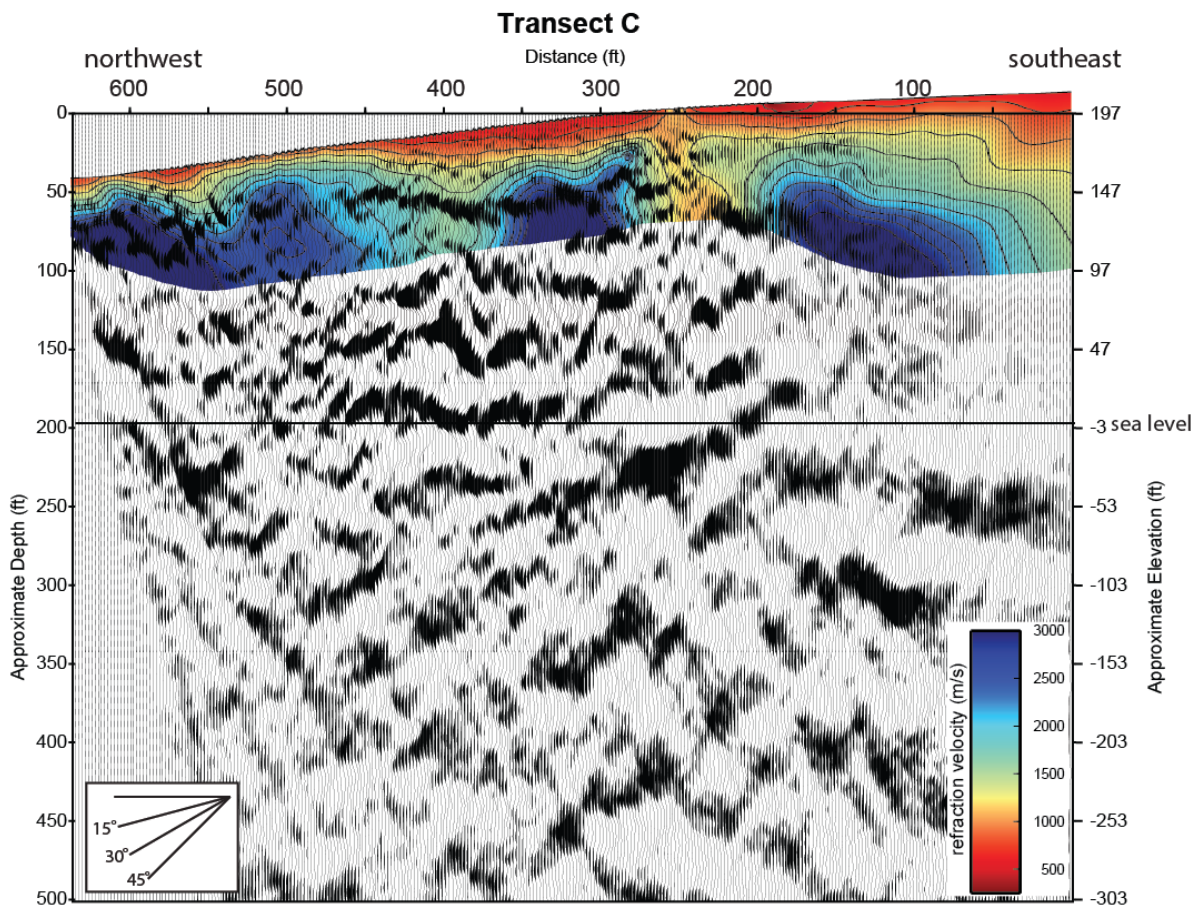
- 1 Transect C
- 2 The 700 foot long northwest-southeast trending Transect C seismic survey was acquired with land
- 3 streamer geophones and PEG-40 seismic source on the Queen Emma quarry access road immediately
- 4 south of North Halawa Valley (Figures 1 and 2). The profile gradually decreases in surface elevation by
- 5 about 60 feet to the northwest (Figure 11). Ko’olau volcanic series basalt outcrops are mapped
- 6 immediately adjacent to the profile (Sherrod et al., 2007) and the North Halawa stream and H3 highway
- 7 are located north of the profile termination.



8 Figure 11. Northwest to southeast Transect C refraction results. (top) Derivative weight sum profile showing ray density for the refraction analysis. (middle) Inversion result showing velocity distribution along the profile. (bottom) Lithologic interpretation derived from velocity profile and from other published results from Hawaii.

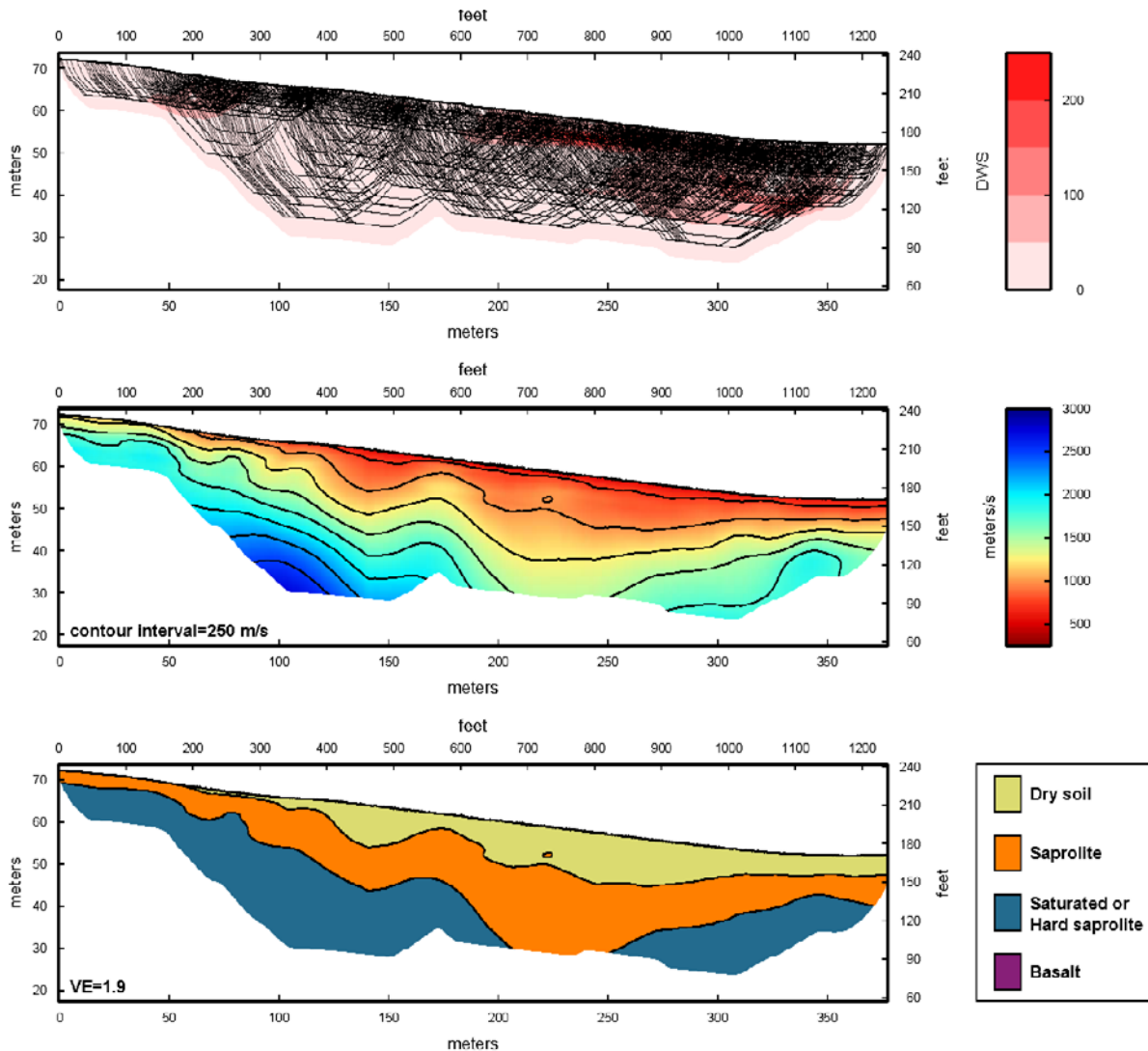
1 The seismic refraction results from Transect C show low seismic velocities in the near surface depths  
 2 with a large velocity gradient that is consistent with shallow saprolite and basalt. With the exception of  
 3 the far southeastern portion of the profile, we identify hard saprolite and basalt within 50 feet of the  
 4 land surface. This result suggests that the basalt outcrops adjacent to the profile are highly weathered  
 5 and are consistent with the velocity of hard saprolite. The southern portion of the profile shows a  
 6 thicker section of alluvium and greater depth to saprolite.

7 The seismic reflection profile shows a reflector at about 50 feet below land surface along the middle  
 8 portions of the profile (Figure 12). This reflector is consistent with the depth to basalt as mapped with  
 9 seismic refraction data. Other deeper reflectors mapped on the profile may represent deeper  
 10 boundaries flow, but there is no continuous reflectivity across the profile to point to laterally continuous  
 11 basalt sub-flow stratigraphy.



12 Figure 12. Transect C reflection and refraction profile showing shallow saprolite and basalt, consistent with mapped geology. Datum elevation is 197 feet.

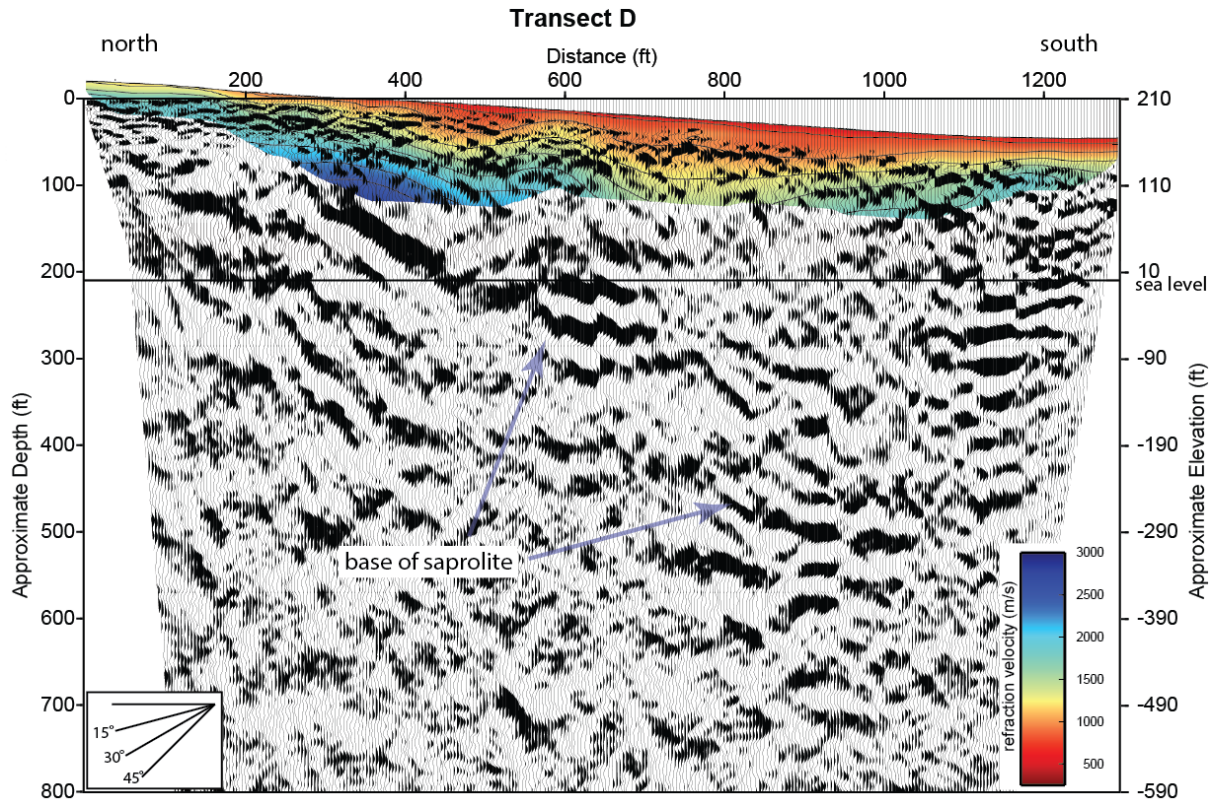
- 1 Transect D
- 2 The 1,250 ft long north-south trending Transect D seismic survey was acquired with land streamer
- 3 geophones and PEG-40 seismic source on Halawa Valley Street in front of the Halawa Correctional
- 4 Facility in South Halawa Valley (Figures 1 and 2). The profile gradually decreases in surface elevation by
- 5 approximately 70 feet to the south (Figure 13). Ko’olau volcanic series basalt outcrops are mapped
- 6 immediately north of the profile on the Queen Emma quarry property (Sherrod et al., 2007). South
- 7 Halawa Stream crosses at approximately position 1200 on this profile, along the southern margin of the
- 8 asymmetric South Halawa Valley.



9 Figure 13. North to south Transect D refraction results. (top) Derivative weight sum profile showing ray density for the refraction analysis. (middle) Inversion result showing velocity distribution along the profile. (bottom) Lithologic interpretation derived from velocity profile and from other published results from Hawaii.

1 The seismic refraction results from Transect D show shallow velocities consistent with saprolite along  
2 the northern portions of the profile and velocities consistent with dry alluvium along the southern 1,000  
3 feet of the profile (Figure 13). The alluvium layer is thickest between transect positions 800 to 900 feet,  
4 and gradually thins to the north and south. This alluvium base geometry is consistent with an  
5 abandoned or broad paleochannel of South Halawa Stream across the center portions of the profile. At  
6 depths upwards of approximately 30 feet, velocities increases are consistent with a transition from  
7 alluvium to dry saprolite and at depths that range from approximately 10 to 100 feet, velocity increases  
8 suggest hard or saturated saprolite are present. It is possible that the higher velocities along the  
9 southern portions of this profile represent perched water derived from the South Halawa Stream and  
10 that the higher velocity saprolite values along the northern portions of this profile are related to more  
11 competent basalt that is seen in outcrop to the north (as seen on Transect C).

12 Immediately below the depth that hard saprolite is mapped along the northern portions of the seismic  
13 refraction profile (Figure 13), the seismic reflection profile shows a high amplitude approximately 30  
14 degree south dipping reflector that is interpreted as the base of saprolite or top of unaltered basalt  
15 (Figure 14). This strong amplitude reflector suggests there is an abrupt seismic velocity and/or rock  
16 density contrast at this boundary along the northern half of the profile that extends to approximately 40  
17 feet below sea level. Farther south (between 800 to 1100-foot distance), the highest amplitude  
18 reflectors extend to depths of about 300 feet below sea level. At the very southern termination of the  
19 profile, high amplitude reflectors shallow and extend from sea level to about 100 feet below sea level. If  
20 the interpreted highest amplitude reflector along the profile represents the base of saprolite, this  
21 suggests that the basalt chemical weathering front advances in a complex manner that may be related  
22 to fluid interactions or basalt stratigraphy. The greatest depth to the asymmetric base of saprolite  
23 reflector coincides with the location of South Halawa Stream.



1 Figure 14. Transect D reflection and refraction profile showing saprolite base reflectors in an asymmetric basin geometry. Datum elevation is 210 feet.

1 Transect E

2 The 250 foot long north-south trending Transect E seismic survey was acquired with planted geophones  
3 and PEG-40 and sledge hammer seismic sources on a perimeter road behind the Halawa Correctional  
4 Facility in South Halawa Valley (Figures 1 and 2). The profile gradually decreases in surface elevation by a  
5 few feet to the south (Figure 15). Ko’olau volcanic series basalt outcrops are mapped within 500 feet  
6 both to the north and south of the profile (Sherrod et al., 2007). Monitoring well 3-2253-03 is located  
7 approximately 50 feet to the east of the 50 foot surface position where alluvium was mapped to a depth  
8 of approximately 80 feet, weathered basalts (saprolite) were interpreted to approximately 320 feet  
9 below land surface, and groundwater was interpreted to be at approximately 210 feet below land  
10 surface (AECOM). South Halawa Stream crosses immediately to the south of this profile.

11 The seismic refraction results from Transect E show velocities consistent with dry alluvium for the upper  
12 5 to 15 feet along the profile (Figure 15). The alluvium layer is thickest at the southern end of the profile  
13 near South Halawa Stream. Below the alluvium, velocity increases are consistent with saprolite. Higher  
14 velocity materials are mapped along the southern half of the profile, consistent with saturated or harder  
15 saprolite. Given the proximity of this portion of the profile to the stream, we infer that these higher  
16 seismic velocities represent the depth to perched water. The depth to water-saturated saprolite on the  
17 northern portions of the profile are greater than the imaging capabilities of the refraction data,  
18 consistent with deeper water table measured in monitoring well 3-2253-03.

19 The seismic reflection profile shows an undulating reflector that ranges in depth from 50 to 100 feet.  
20 This reflector is interpreted to represent the base of alluvium, consistent with a depth of 80 feet in the  
21 nearby monitoring well 3-2253-03 (80 foot depth). This depth is greater than the 1,000 m/s contour  
22 identified with refraction analyses, suggesting that alluvium seismic velocities may be faster than  
23 published reports from Hawaii and overlap with velocity ranges for highly altered saprolite. Two strong  
24 amplitude flat-lying reflectors at 250 and 330 ft below land surface were identified and the deeper  
25 reflector is interpreted to represent the saprolite base. This is consistent with the lithologic log  
26 interpretation for dense gray basalt overlying weathered basalt at this depth. Due to the short length of  
27 the seismic profile, the geometry of saprolite base is poorly constrained.

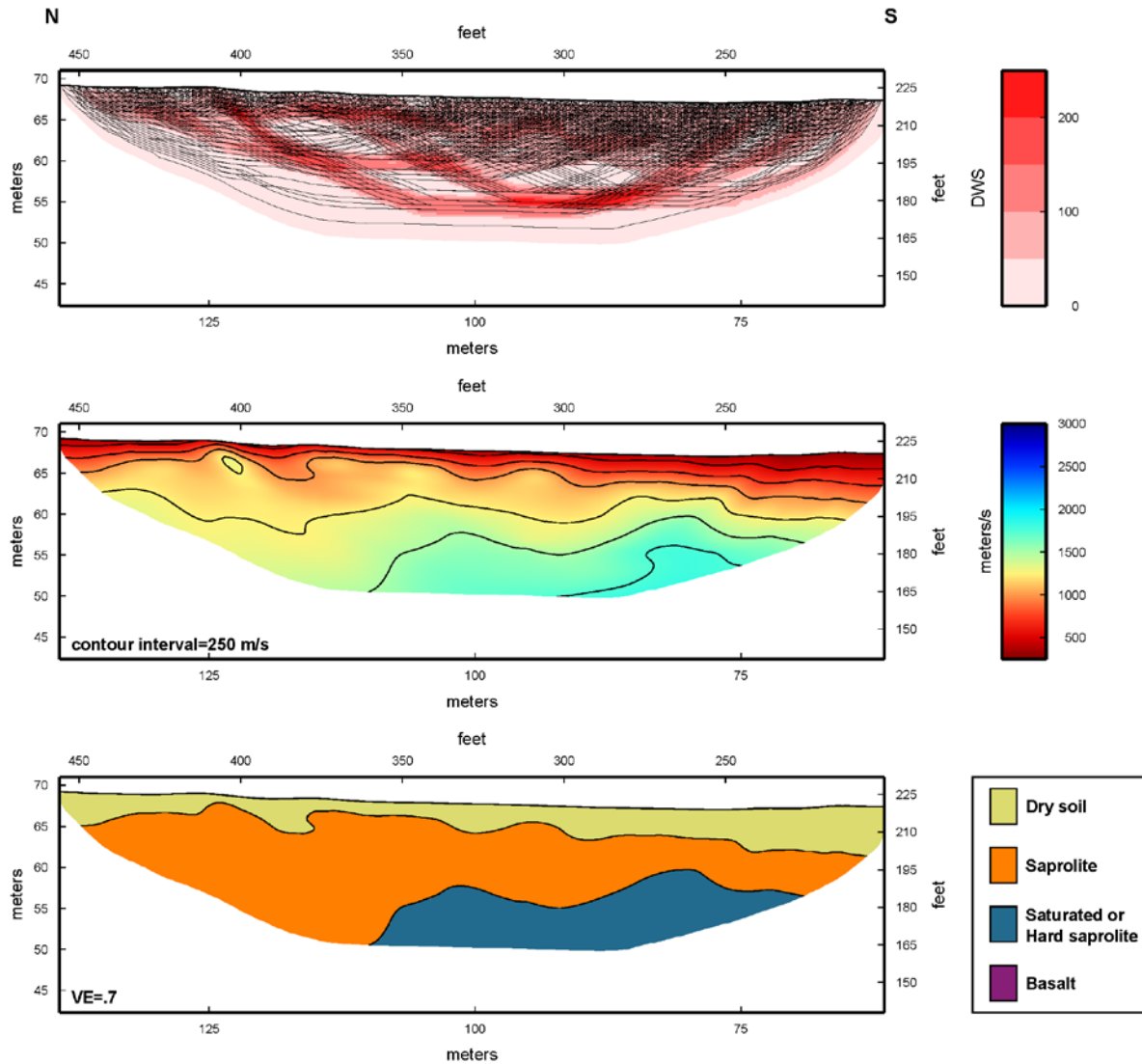


Figure 15. North to south Transect E refraction results. (top) Derivative weight sum profile showing ray density for the refraction analysis. (middle) Inversion result showing velocity distribution along the profile. (bottom) Lithologic interpretation derived from velocity profile and from other published results from Hawaii.

1

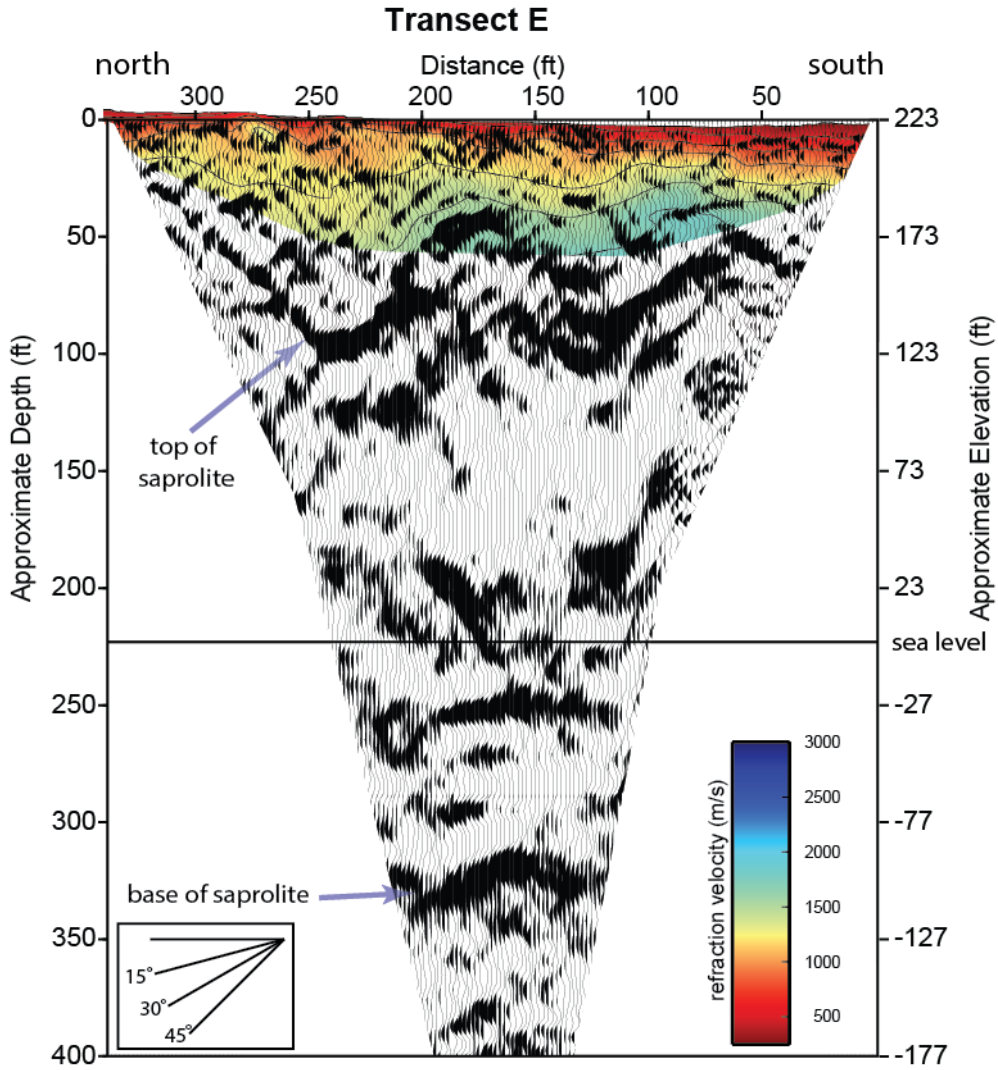
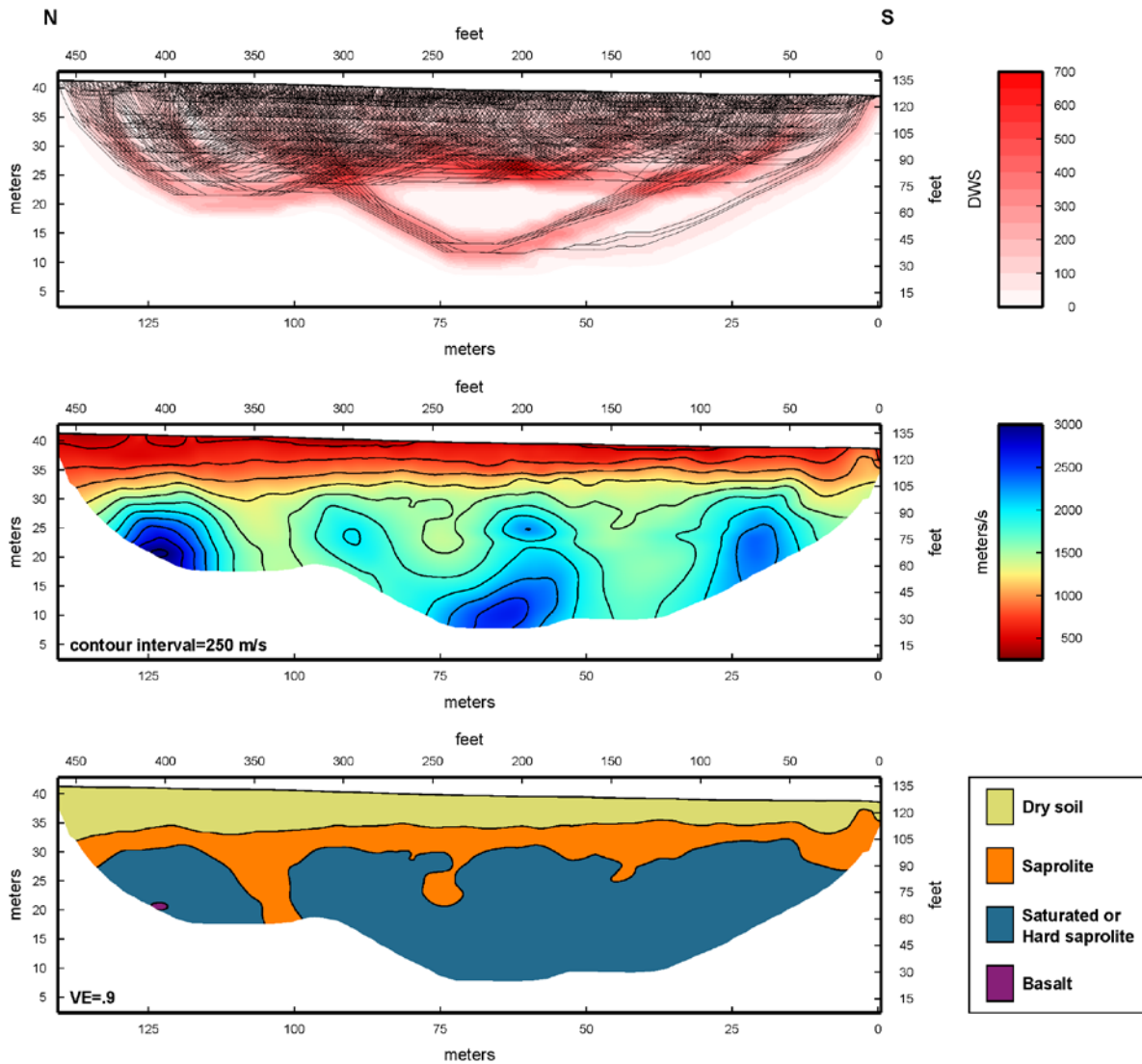


Figure 16. Transect E reflection and refraction profile showing an undulating reflection that is interpreted as top of saprolite. The deepest identified flat-lying reflector is interpreted to represent base of saprolite. This depth is consistent with lithologic logs from nearby boreholes. Datum elevation is 223 feet.

1

- 1 Transect F
- 2 The 450 foot long north-south trending Transect E seismic survey was acquired with planted geophones
- 3 and PEG-40 seismic source along an access road within the Hawaii Department of Agriculture Animal
- 4 Quarantine Station facility in South Halawa Valley (Figures 1 and 2). The profile decreases in surface
- 5 elevation by a few feet to the south (Figure 17). South Halawa Stream is located just south of this profile
- 6 near the southern margin of the valley. Honolulu volcanic series rocks are mapped about 100 feet south
- 7 of the profile and Ko’olau volcanic series rocks are mapped to the north of the profile.



8 Figure 17. North to south Transect F refraction results. (top) Derivative weight sum profile showing ray density for the refraction analysis. (middle) Inversion result showing velocity distribution along the profile. (bottom) Lithologic interpretation derived from velocity profile and from other published results from Hawaii.

1 The seismic refraction results from Transect F show velocities consistent with dry alluvium for the upper  
2 15 to 25 feet along the profile (Figure 17). The alluvium layer increases in thickness to the north. Below  
3 the alluvium, velocity increases are consistent with saprolite and saturated/hard saprolite along most of  
4 the profile. Given the proximity of this portion of the profile to the South Halawa Stream and the  
5 relative uniformity to the top of hard/saturated saprolite, it was interpreted that these higher seismic  
6 velocities represent the depth to a perched water system. Velocities representing basalt are either at  
7 the bottom of the refraction model or, at greater depths.

8 The seismic reflection profile shows a relatively flat lying reflector at approximately 80 to 100 foot  
9 depths that may represent top of saprolite or water table reflector. This reflector is deeper than the  
10 interpreted alluvium base mapped with refraction methods. A 10 degree south dipping reflector at 400  
11 to 500 foot depth below land surface is interpreted as the base of saprolite. Considering the relative  
12 position of this reflector with respect to the extent of South Halawa Valley, it is interpreted that the  
13 saprolite base contains an asymmetric bedrock geometry where the greatest base of saprolite depth is  
14 located south of the Transect F limits. This saprolite base geometry is consistent with Transect D depths  
15 and inferred bedrock geometry. This observation supports a more active chemical weathering front  
16 beneath the lowest elevations across the valley and beneath the present day South Halawa Stream.

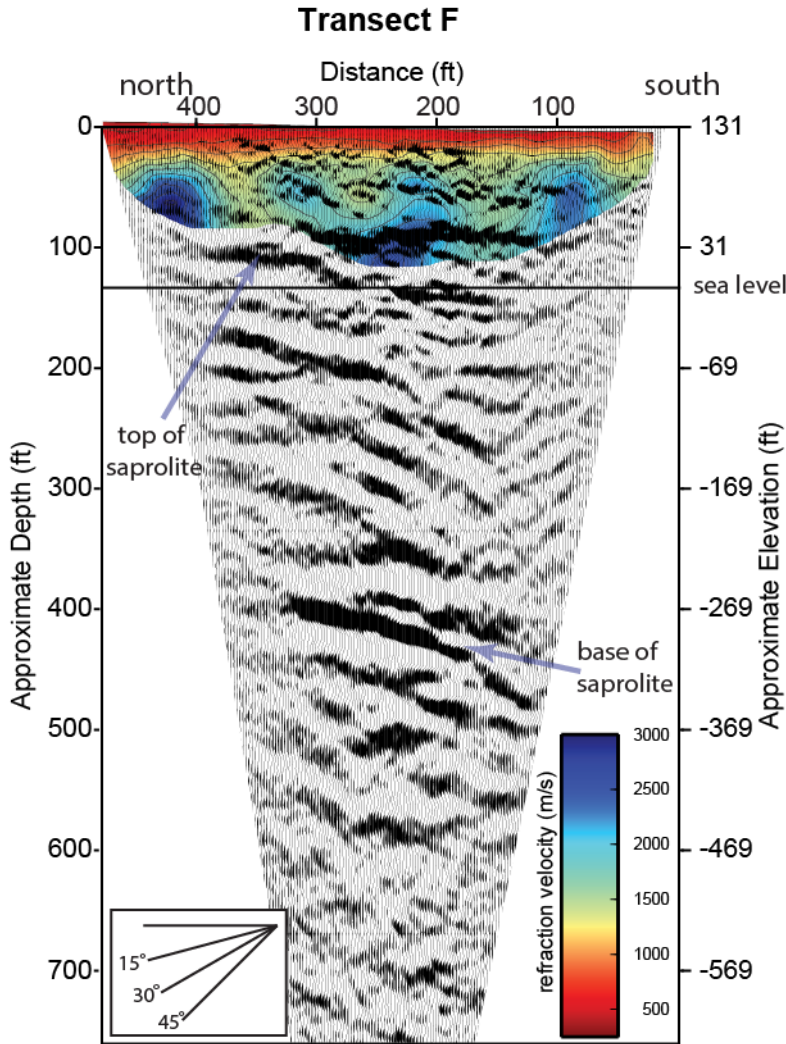


Figure 18. Transect F reflection and refraction profile showing a near flat-lying reflector that is interpreted as top of saprolite at a depth of approximately 100 feet. We define a south-dipping reflector at a depth of approximately 400 feet to represent the base of saprolite. This depth is consistent with lithologic logs from nearby boreholes. Datum elevation is 131 feet.

1

1 Transect G

2 The 3,000 foot long northeast-southwest trending Transect G seismic survey was acquired with land  
 3 streamer geophones and PEG-40 seismic source on Icarus Way on the Navy’s Red Hill property (Figures 1  
 4 and 2). The profile gradually decreases in surface elevation by about 100 feet to the west (Figure 19).  
 5 Ko’olau volcanic series basalt outcrops are mapped immediately south of the profile along Red Hill  
 6 (Sherrod et al., 2007). Monitoring wells RHMW06 and RHMW07 are located along the profile at about  
 7 positions 180 and 1320 respectively (Figures 1 and 20) and show alluvium over saprolite at 24 foot and  
 8 23 foot depths, saprolite over basalt at 35 feet and 27 feet, and depth to water table at 239 and 192 feet  
 9 respectively.

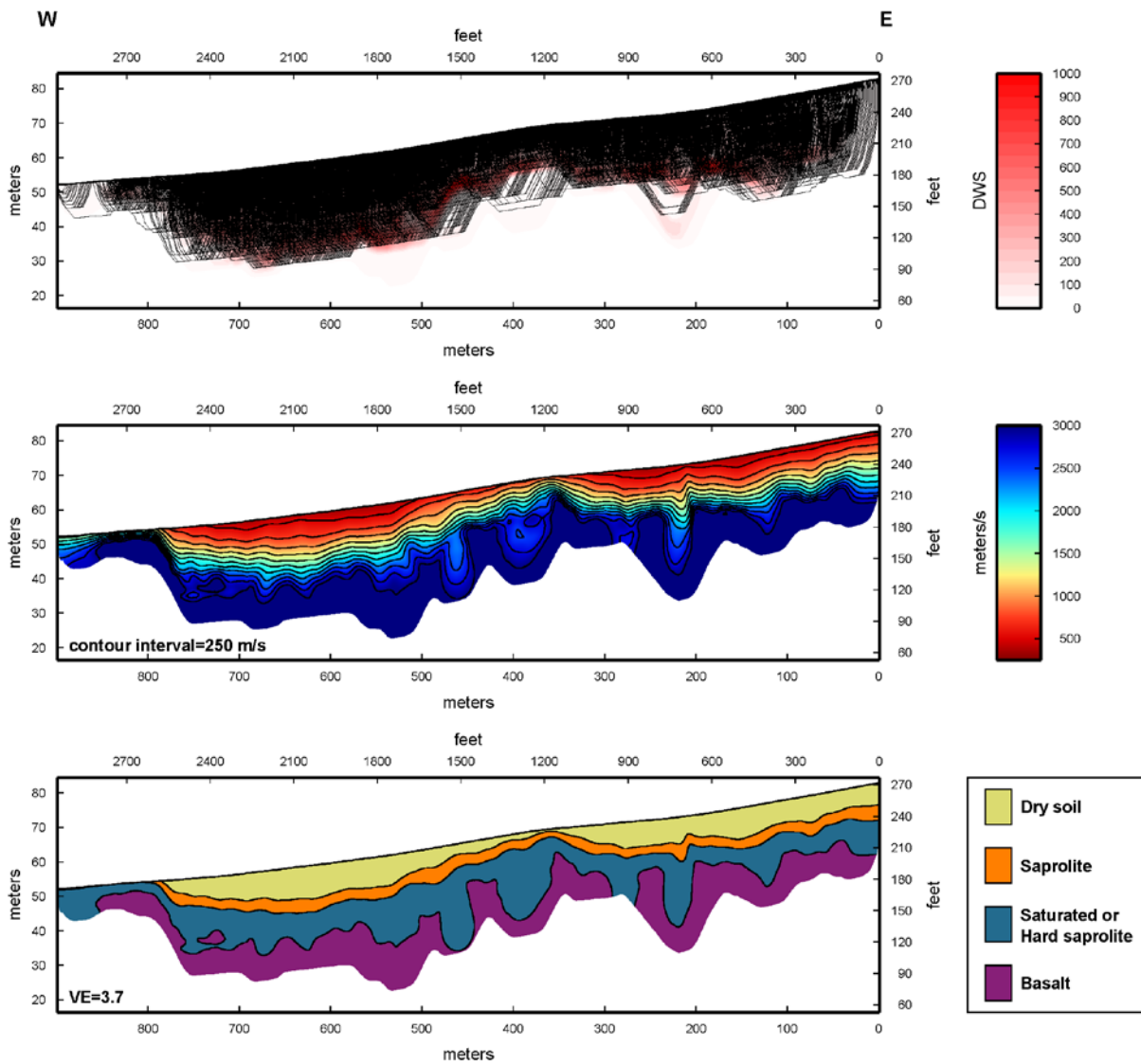
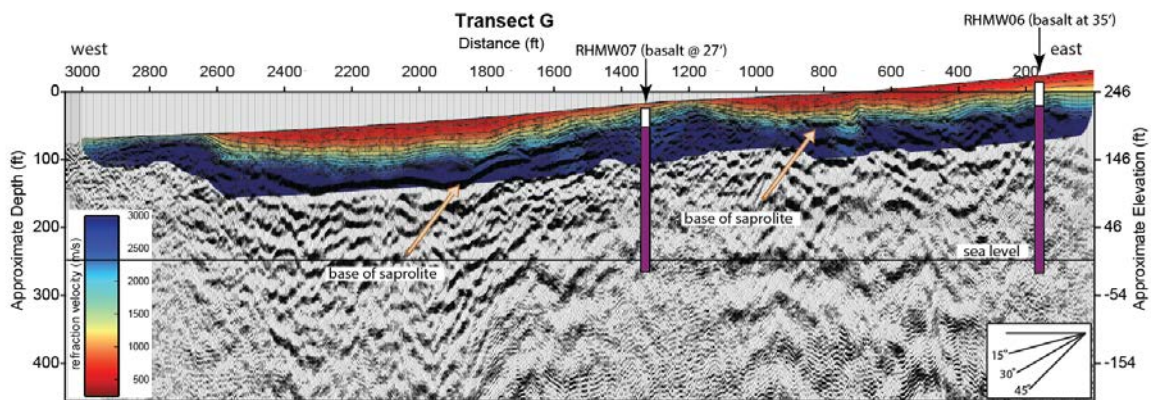


Figure 19. West to east Transect G refraction results. (top) Derivative weight sum profile showing ray density for the refraction analysis. (middle) Inversion result showing velocity distribution along the profile. (bottom) Lithologic interpretation derived from velocity profile and from other published results from Hawaii.

10

1 The seismic refraction results from Transect G show velocities consistent with dry soil or alluvium for the  
 2 upper 0 to 30 feet along the profile (Figure 19). Deeper pockets of dry alluvium are observed between  
 3 400 to 1500 feet along the transect between positions 1900 and 2800 feet. The western and central  
 4 portion of the profile show faster velocities at the land surface, consistent with saturated or hard  
 5 saprolite. Below the alluvium, velocity increases are mostly consistent with saturated/hard saprolite  
 6 along the most of the profile. The depth to saprolite base determined from the refraction results is very  
 7 consistent with lithologic contacts derived from monitoring well logs. These monitoring wells show  
 8 greater depths to water, thus we conclude that the saprolite and shallow basalts are dry

9 The seismic reflection image for Transect G (Figure 20) shows a strong reflector that is consistent in  
 10 depth to the saprolite base. Where the refraction results show basalt approaching land surface, the  
 11 saprolite base reflection is attenuated. This is mostly due to the limited reflection coverage (fold) in the  
 12 upper 20 feet of the profile related to the lack of geophone coverage at distances less than 30 feet.



13 Figure 20. Transect G reflection and refraction profile showing a reflector at the base of saprolite,  
 consistent with the transition in seismic velocities to unaltered basalt. Two monitoring wells are  
 located near this profile and are used to constrain geologic interpretations. Datum elevation is 246  
 feet.

1 Transect H  
2 The 830 foot long west-east trending Transect H seismic survey was acquired with planted geophones  
3 and mostly sledge hammer seismic sources across the Moanalua golf course (Figures 1 and 2). A few  
4 PEG40 hammer hits were acquired along the east end of the profile, off of driving ranges and greens.  
5 The profile decreases in surface elevation by about 60 feet to the east (Figure 15) and much of the  
6 profile was acquired along a topographic saddle between golf course holes. The Moanalua Stream is  
7 located immediately east of the profile. Honolulu volcanic series basalt outcrops are mapped at the  
8 surface along the western portions of the profile and Ko'olau volcanic series basalts are mapped  
9 immediately to the north of the profile. (Sherrod et al., 2007). In the center of the profile, rock outcrops  
10 consistent with saprolite were noted.

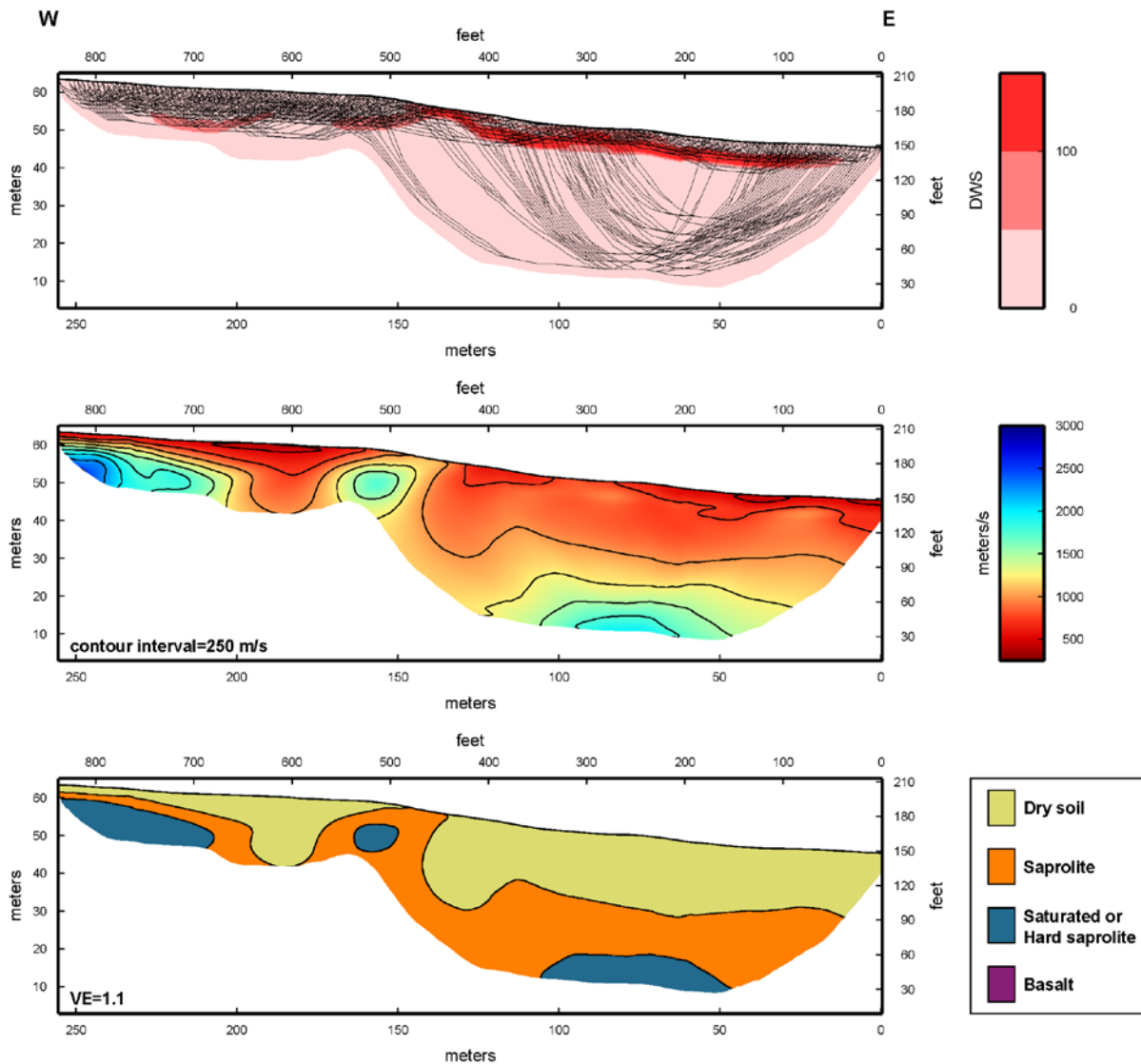
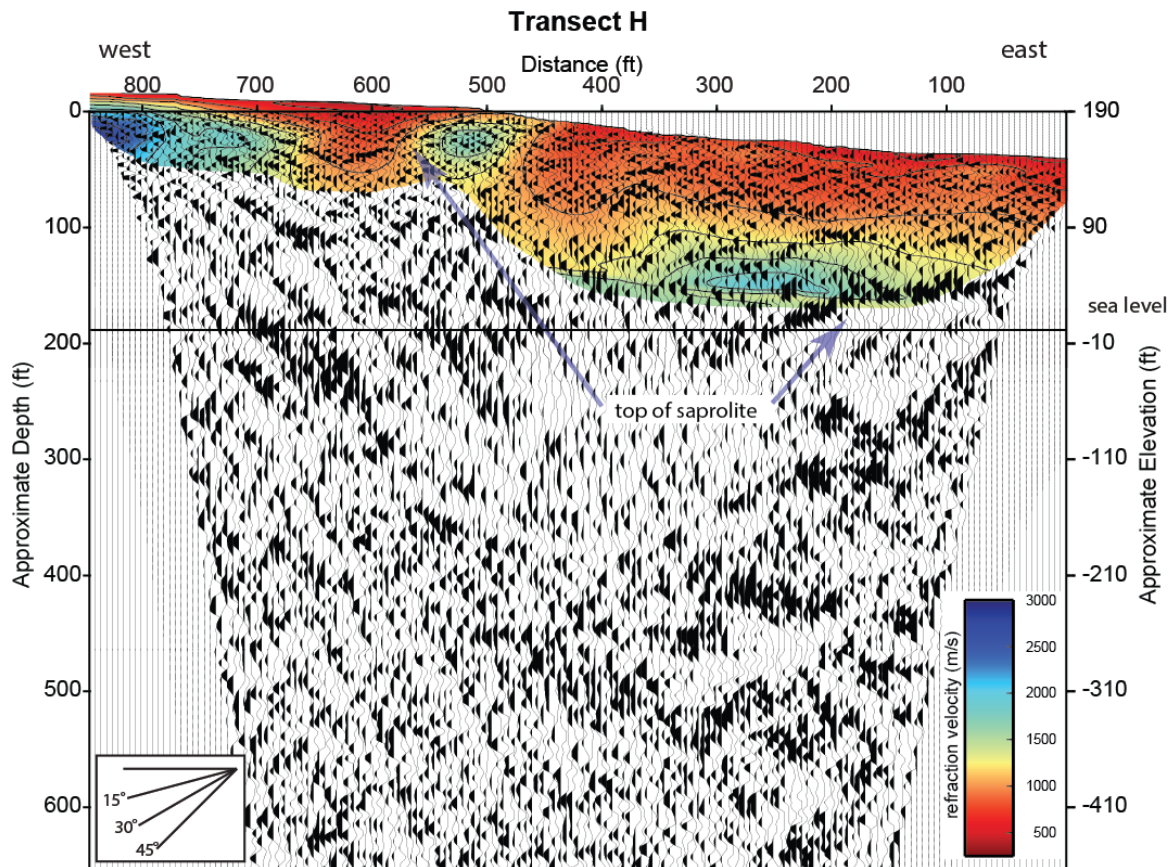


Figure 21. West to east Transect H refraction results. (top) Derivative weight sum profile showing ray density for the refraction analysis. Note the deeper arrivals from the PEG40 hammer hits. (middle) Inversion result showing velocity distribution along the profile. (bottom) Lithologic interpretation derived from velocity profile and from other published results from Hawaii.

1

2 The seismic refraction results from Transect H show velocities consistent with dry alluvium for the upper  
 3 60 feet along the eastern portion of the profile and variable depths along the western portion of the  
 4 profile (Figure 21). Refraction arrivals from greater depths along the eastern portion of the profile  
 5 resulted from PEG40 hits. The thick alluvium layer beneath the eastern half end of the profile is  
 6 consistent with mobilized sediment from the Moanalua Stream (paleochannel). Below alluvium,  
 7 refraction velocity increases are consistent with the presence of saprolite. Saprolite velocities are  
 8 mapped to surface elevations in the middle of the profile where weathered rock outcrops appear (noted  
 9 on field observations). The depth to saturated or hard saprolite is within 10 to 20 feet beneath the

1 western portion of the profile and approximately 100 feet beneath the eastern portion of the profile.  
 2 Given the proximity to mapped basalt along the western portions of the profile (Sherrod et al. 2007), we  
 3 presume that the faster velocity materials represent hard saprolite and are likely not saturated.  
 4 The seismic reflection profile for Transect H shows poor quality reflectivity, likely due to the lack of  
 5 PEG40 hammer hits that help produce signals to greater depths (Figure 22). We do observe  
 6 discontinuous reflectors in the upper 200 feet below land surface that we interpret as top of saprolite.  
 7 However, the refraction data better constrain this contact. We do not observe a deeper reflection that is  
 8 consistent with depth to saprolite base. Here, it is believed that more seismic energy is needed to image  
 9 this contact.



10 Figure 22. Transect H reflection and refraction profile showing a reflector at the top of saprolite,  
 11 consistent with the transition in seismic velocities to saprolite. Saprolite is observed at the surface in  
 12 the center of the profile. Datum elevation is 190 feet.

11 Transect I

12 The 350 foot long north-south trending Transect I seismic survey was acquired with planted geophones  
 13 and PEG40 seismic hammer sources across the eastern extent of the Moanalua golf course (Figures 1  
 14 and 2). The profile decreases in surface elevation by a few feet to the south (Figure 24). The Moanalua  
 15 Stream is located immediately south of the profile. Honolulu volcanic series basalt outcrops are mapped  
 16 at the surface to the west of the profile and Ko’olau volcanic series basalts are mapped immediately to

- 1 the north of the profile (Figure 2; Sherrod et al., 2007). Older alluvium is mapped at the surface along
- 2 the length of the profile.

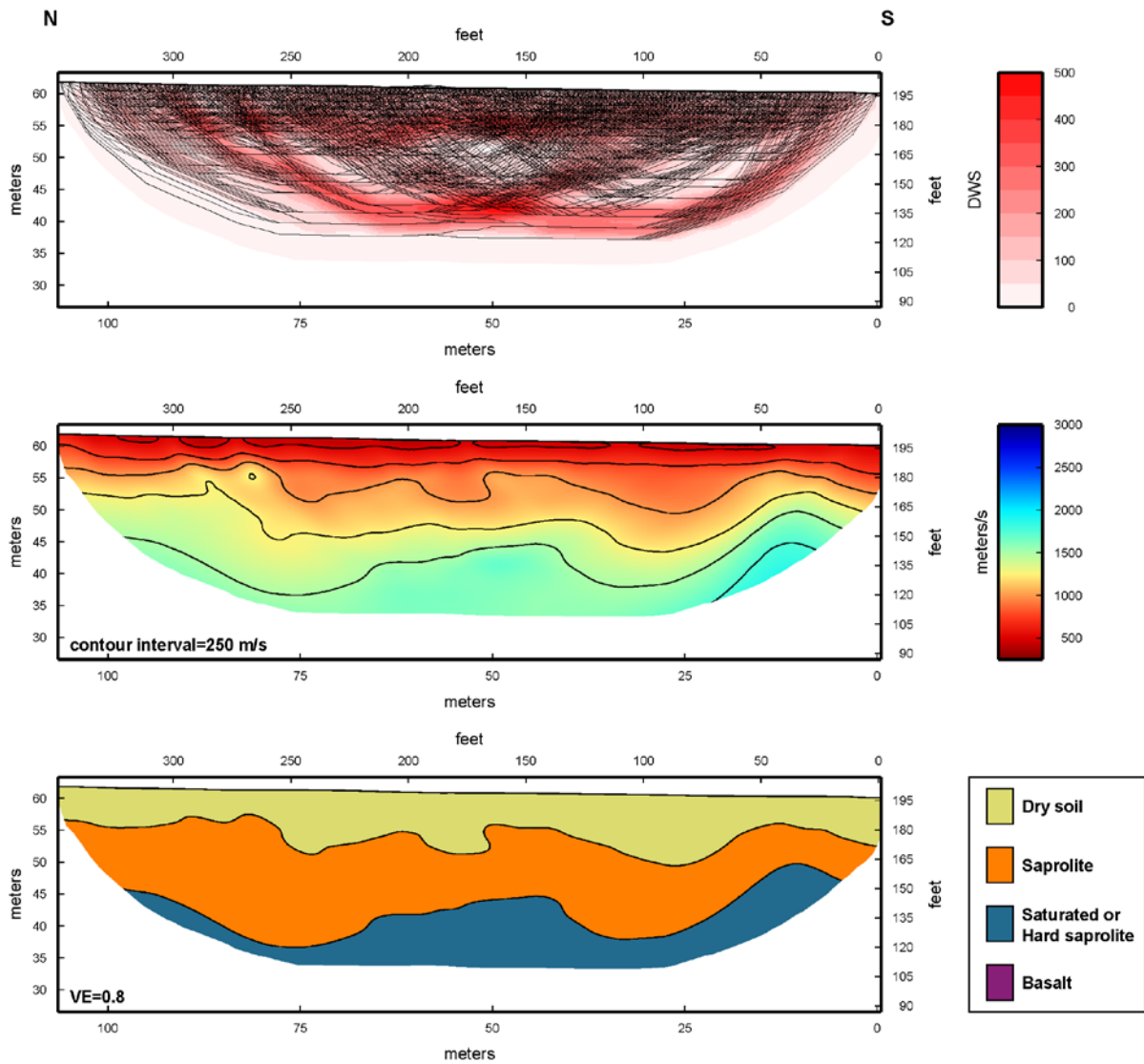


Figure 23. West to east Transect I refraction results. (top) Derivative weight sum profile showing ray density for the refraction analysis. (middle) Inversion result showing velocity distribution along the profile. (bottom) Lithologic interpretation derived from velocity profile and from other published results from Hawaii.

- 3
- 4 The seismic refraction results from Transect I show velocities consistent with dry alluvium for the upper
- 5 20 to 30 feet along the length of the profile (Figure 21), consistent with mobilized sediment from the
- 6 Moaualua Stream (paleochannel). Below the alluvium, velocity increases are consistent with saprolite.
- 7 Along the length of the profile, refraction velocities gradually increase and are consistent with hard or

- 1 saturated saprolite at depths of approximately 50 to 80 feet. The depth to saturated sediments in not
- 2 constrained is in this valley.
- 3 The seismic reflection profile for Transect I shows a continuous reflector at a depth of approximately 50
- 4 feet which is consistent with the base of alluvium (slightly deeper than the 1,000 m/s contour that we
- 5 use for refraction breaks) (Figure 24). An arcuate reflector at a depth of approximately 250 to 300 feet
- 6 may represent the base of saprolite, but this reflector was poorly imaged due to the short line length.

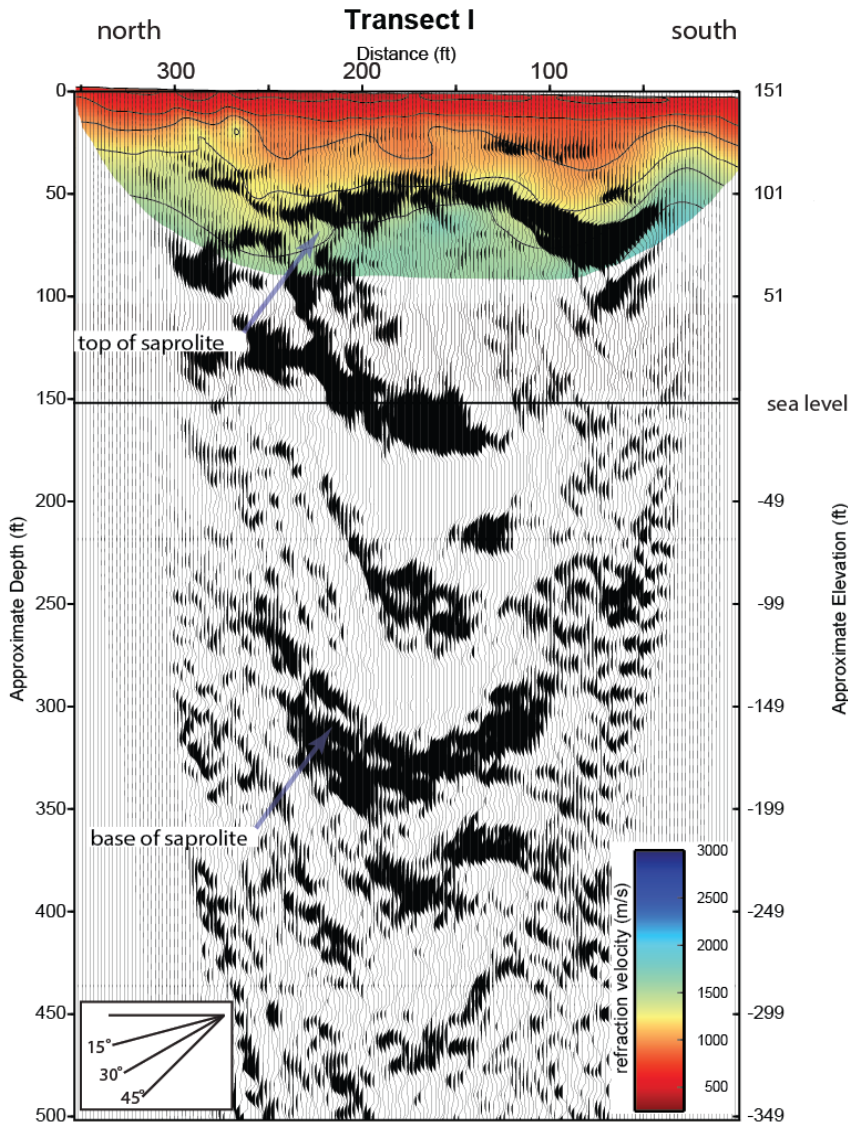


Figure 24. Transect I reflection and refraction profile showing a reflector at the top of saprolite, consistent with the transition in refraction velocities from alluvium to saprolite. A deeper arcuate reflector may represent the base of saprolite, but this reflector is poorly imaged beneath the ends of the profile. Datum elevation is 151 feet.

7

1 Conclusions

2 The Red Hill seismic survey yielded information on key hydrostratigraphic boundaries below three  
3 valleys on the island of O’ahu, Hawaii. The seismic velocity and reflection results from this study, allow  
4 definition of four hydrostratigraphic units. Seismic velocities that are consistent with dry alluvium, as  
5 measured by seismic velocities less than 1,000 m/s, extend up to 60 feet deep in all three valleys. These  
6 shallow alluvial sediments overlie saprolite, as defined by velocities between 1,000-1,500 m/s. The  
7 thickness of dry saprolite layer ranges from 0 to 100 feet thick. With increasing depth and rock density,  
8 saprolite increases in seismic velocity to greater than 1,500 m/s. Also, with saturation, seismic velocities  
9 in both alluvium and saprolite exceed 1,500 m/s. These zones extend in depth for a few hundred feet  
10 beneath all three valleys. Unaltered basalts exceed a seismic velocity of 3,000 m/s. These velocities are  
11 observed along the valley margins and at depth beneath each valley. We find highly weathered volcanic  
12 rocks extend to about 300 feet below sea level beneath depths North Halawa and South Halawa valleys.  
13 The depth and saprolite base geometry is less constrained beneath Moanalua Valley. The greatest depth  
14 to saprolite base is consistent with the surface expression of the streams that drain the valleys.

## 1 References

- 2 AECOM Technical Services, Inc. (2017). Final Fourth Quarter 2017 Quarterly GW Monitoring Report, Red  
3 Hill Bulk Fuel Storage Facility, JBPHH, O’ahu, Hawaii.
- 4 Brandes, H. G., Robertson, I. N., & Johnson, G. P. (2010). Soil and rock properties in a young volcanic  
5 deposit on the island of Hawaii. *Journal of Geotechnical and Geoenvironmental Engineering*, 137(6), 597-  
6 610.
- 7 Deregowski, S. M. (1986) What is DMO?: *First Break*, 4, 7.
- 8 Hale, D., 1988, Dip moveout processing - course notes: SEG Continuing Education.
- 9 Gulunay, N. (1986) F-X Decon and the Complex Weiner Prediction Filter for Random Noise Reduction on  
10 Stacked Data, paper presented at the Society of Exploration Geophysicists 56th Annual International  
11 Meeting, Houston, TX.
- 12 Hunt Jr. C.D. (1996) Geohydrology of the Island of Oahu, Hawaii. *U.S. Geological Survey Professional*  
13 *Paper*. pp. 1412-B, B1–B54.
- 14 Izuka, S. K. (1992). Geology and stream infiltration of North Halawa Valley, Oahu, Hawaii (No. 91-4197).  
15 Geological Survey (US).
- 16 Izuka, S. K., J. A. Engott, M. Bassiouni, A. G. Johnson, L. D. Miller, K. Rotzoll, and A. Mair. (2016) Volcanic  
17 Aquifers of Hawai’i—Hydrogeology, Water Budgets, and Conceptual Models. Scientific Investigations  
18 Report 2015–5164. Water Availability and Use Science Program. *U.S. Geological Survey*.
- 19 Liberty, L. (2011). Hammer seismic reflection imaging in an urban environment. *The Leading Edge*, 30(2),  
20 146-153.
- 21 Liberty, L. M., Schmitt, D. R., & Shervais, J. W. (2015). Seismic imaging through the volcanic rocks of the  
22 Snake River Plain: insights from Project Hotspot. *Geophysical Prospecting*, 63(4), 919-936.
- 23 Mavko, G., Mukerji, T., & Dvorkin, J. (2009). The rock physics handbook: Tools for seismic analysis of  
24 porous media. Cambridge university press.
- 25 Nelson, S. T., Tingey, D. G., & Selck, B. (2013). The denudation of ocean islands by ground and surface  
26 waters: The effects of climate, soil thickness, and water contact times on Oahu, Hawaii. *Geochimica et*  
27 *Cosmochimica Acta*, 103, 276-294.
- 28 Pelton, J. R. (2005). Near-surface seismology: Surface-based methods. In *Near-Surface Geophysics:*  
29 *Society for Exploration Geophysicists volume IG #13, Butler, D. K. editor*, 219-263.
- 30 Ronen, J., and J.F. Claerbout (1985) Surface-consistent residual static corrections by stack power  
31 maximization: *Geophysics*, 50, 2759-2767.
- 32 Sherrod, D. R., Sinton, J. M., Watkins, S. E., & Brunt, K. M. (2007). Geologic map of the State of Hawaii.  
33 US Geological Survey Open-File Report, 1089, 83.
- 34 Stanchits, S., Vinciguerra, S., & Dresen, G. (2006). Ultrasonic velocities, acoustic emission characteristics  
35 and crack damage of basalt and granite. *Pure and Applied Geophysics*, 163(5-6), 975-994.

- 1 St. Clair, J. (2015). Geophysical investigations of underplating at the Middle American Trench,  
2 weathering in the critical zone, and snow water equivalent in seasonal snow, PhD thesis, Univ. of  
3 Wyoming.
- 4 Van der Veen, M. and Green, A.G., 1998. Land streamer for shallow data acquisition: evaluation of  
5 gimbal-mounted geophones. *Geophysics*, 63, 1408-1413.
- 6 Van der Veen, M. Spitzer, R., Green, A.G., and Wild, P., 2001. Design and application of a towed land-  
7 streamer for cost-effective 2D and pseudo-3D shallow seismic data acquisition. *Geophysics*, 66, 482-500.
- 8 Vidale, J. (1988) Finite-difference Calculation of Travel Times: *Bulletin of the Seismological Society of*  
9 *America*, 78, 2062-2076.
- 10 Von Voigtlander, J. (2015). P-wave velocity of weathering profiles from a basalt climosequence:  
11 Implications for weathering on the mechanical properties of the critical zone, Master in Earth and  
12 Environmental Science, University of Michigan.
- 13 Von Voigtlander, J., Clark, M. K., Zekkos, D., Greenwood, W. W., Anderson, S. P., Anderson, R. S., & Godt,  
14 J. W. (2018) Shallow seismic profiles reveal anisotropy in critical zone architecture linked to weathering  
15 threshold. *Earth Surface Processes and Landforms*.
- 16 Yaede, J. R., McBride, J. H., Nelson, S. T., Park, C. B., Flores, J. A., Turnbull, S. J., ... & Gardner, N. L.  
17 (2015). A geophysical strategy for measuring the thickness of the critical zone developed over basalt  
18 lavas. *Geosphere*, 11(2), 514-532.
- 19 Yilmaz, O. (2001). *Seismic Data Analysis: Processing, Inversion, and Interpretation of Seismic Data*,  
20 Society of Exploration Geophysicists, Tulsa IG#10 series, Oklahoma, 2027 pp.
- 21 Zelt, C. A., Haines, S., Powers, M. H., Sheehan, J., Rohdewald, S., Link, C., Hayashi, K., Zhao, D., Zhou, H.,  
22 Burton, B. L., Petersen, U. K., Bonal, N. D., & Doll, W. E., 2013. Blind test of methods for obtaining 2-D  
23 near surface seismic velocity models from first-arrival traveltimes, *Journal of Environmental and*  
24 *Engineering Geophysics*, 18, 183-194, DOI:10.2113/JEEG18.3.183.